OES 10th Semester Master Thesis
Report

Membrane Fouling Modeling and enhancement through gas injection

Submitted in partial fulfillment for the degree of

Master of Science
in Offshore and Energy System

Submitted by

Dario Spina

Under the supervision of:
Jens Muff   Marco Maschietti

AALBORG UNIVERSITY
DENMARK

Energy Department
AALBORG UNIVERSITY
Niels Bohrs Vej 8, 6700 Esbjerg

Title:

Membrane Fouling Modeling and Enhancement through gas injection

Semester:

10^{th}

Project period:

02/2016 - 9/06/2016

ECTS:

30

Supervisor:

Jens Muff

Marco Maschietti

Project group:

OES10 – 5

Synopsis:

In the following thesis it is analyzed membrane technology in produced water and in particular, the use of gas-injection inside the feed to reduce the fouling phenomena into a cross flow tubular filtration.

An existing model for the permeate flux decline with pure water will be experimentally validated and through the use of a membrane setup and CFD simulations.

The same model will be used with output results from CFD simulations of feed water with gas injection. The performances will be discussed and also the values in which this technique would have the highest impact.

Written by:

____

Dario Spina

Number printed: 3

Pages: 64

Appendix: 7

Enclosures: 1 DVD

By signing this document, each member of the group confirms participation on equal terms in the process of writing the project. Thus, each member of the group is responsible for the all contents in the project.

Abstract

The following work focuses on the tubular crossflow membrane filtration and its enhancement through the injection of gas inside the membrane. An existing physical model for crossflow flux decline is presented and validated. The model gives emphasis on the relationship between the permeate flux decline and the wall shear stress. CFD simulations with both one-phase and two-phase flow are made to calculate the wall shear stress. The values obtained are re-inputted into the model, and used to compare the one-phase and the two phase flow. The results show that the steady state flux achieved when the fouling process is higher in a feed flow with gas injection compared to one without. The enhancement is significant also for small injection of gas, which can make the produced water process faster and more efficient. The boundary parameters influencing the output are highlighted in order to understand best conditions for this technology.

Abbreviations

BTEX benzene toluene xylene

CFI Combined Fouling Index

CIP Cleaning in Place

COD Chemical Oxygen Demand

DOC Dissolved Organic Carbon

FDR Flux Decline Rate

MF Micro Filtration

MFI Modified Fouling Index

MIEX Magnetic Ion Exchanger

NF Nano Filtration

NORM Naturally Occurring Radioactive Materials

OSPAR Convention for the Protection of the Marine Environment of the North-East Atlantic

PW Produced Water

RO Reverse Osmosis

SDI Silt Density Index

TDS Total Dissolved Solid

TMP Transmembrane Pressure

TPH Total petroleum hydrocarbon

UF Ultra Filtrationr

WOR Produced Water to Oil Ratio

Contents

List of Figures **v**

1 Introduction **1**

2 Problem formulations **4**

2.1 Delimitation 5

3 Introduction to Membrane Filtration **6**

3.1 Membrane filtration processes 7

3.2 Crossflow vs Dead-end 9

3.2.1 Cross-Flow 11

3.3 Membrane Train 11

3.4 Fouling 11

3.4.1 Backflush 14

3.4.2 Fouling Model: Darcy Law and Important Parameters . . . 15

3.4.3 Fouling Model 20

3.4.4 Influences on Fouling 22

3.4.5 Pretreatments to fouling 25

3.4.6 Membrane Cleaning 26

4 Two Phase flow **27**

4.1 Flow Patterns 27

4.2 Benefits 30

5 Model Description **32**

6 Experiments **35**

6.1 Porosity 35

6.2 Permeability and Membrane Clean Resistance 36

6.3 Produced Water in Crossflow SiC membrane 38

6.3.1 Setup 38

6.3.2 Produced Water Experiment Description 40

6.3.3 Results 42

7 CFD Simulations **45**

7.1 Geometry 46

7.1.1 Mesh 48

7.2 Permeate Flow 48

7.3 Two-phase flow with porous zone 49
7.4 Two-Phase Flow 50
7.4.1 Simulation with 0.1 m/s 51
7.4.2 Simulation with 1 m/s 55
7.4.3 Simulation with 2 m/s 56
7.4.4 Simulation with 4 m/s 56
7.4.5 Results and Discussion 56

8 Results and Discussion 57

8.1 Results 57
8.1.1 Air injection 0.1 m/s 58
8.1.2 Air injection 1 m/s and 2 m/s 59
8.1.3 Air injection 4 m/s 60
8.2 Optimal conditions for the two phase-flow enhancement 61

9 Conclusions 62

Bibliography 64

Bibliography 64

10 Appendix 66

10.1 Appendix A - Permeability and Clean Membrane Resistance 66

10.2 Appendix B - Flux Decline Model 69

10.3 Appendix C - Experimental vs Theoretical Calculation 71

List of Figures

3.1 In the depth filtration particles accumulate inside the material (left), on the surface filtration (right) a cake layer creates on surface . . . 7

3.2 Particle retention for the different filtration processes. From the top to the bottom :NF, UF, MF . . . 9

3.3 Example of dead-end filtration and crossflow filtration . . . 10

3.4 A common application of membranes, combining both membranes in series (vessel) and in parallel. . . . 12

3.5 Three different cases in fouling: a) Membrane pore diameter bigger than particle diameter b) Membrane pore diameter approximately the same size as particle diameter c) particle diameter bigger than membrane pore size . . . 13

3.6 Three phases of the flux decline due to the fouling . . . 14

3.7 Permeate Flux vs Time and effects of backflush operations . . . 15

3.8 Illustration of a 2D flow through a porous media . . . 17

3.9 A)Overview of a porous media in a section parallel to the flow B) Shortest path(X) and the actual flow path (L) . . . 19

3.10 Filtration resistance by the formation of reversible fouling layer after 4 h of filtration at different cross-flow velocities: (a) MF and (b) UF 23

3.11 Pressure vs time graph for : a) Continuous surface shear stress profile. b) Sustained peak surface shear stress profile c) Low peak surface shear stress profile. d) High peak surface shear stress profile. 24

4.1 Different flow patterns for two-phase flow in an vertical pipe 28

4.2 Different flow patterns for two-phase flow in an horizontal pipe . . . 29

4.3 Map for horizontal two phase flow patterns 30

4.4 Map for vertical two phase flow patterns 30

5.1 Front of equilibrium in a finite tubular crossflow representation . . . 33

6.1 TMP vs Permeate Flux 37

6.2 Membrane and membrane housing 38

6.3 Setup Diagram for the experiment 39

6.4 Histogram of the mean particle size for the 0.1 micron latex particles 41

6.5 Three measurements for estimation of the size of the 0.1 micron latex particles 42

6.6 Experimental vs Theoretical Permeate Flux 43

7.1 Geometry number 1 and its Boundary conditions 46

7.2 Geometry number 2 and its Boundary conditions 47

7.3 Geometry number 2 and its Boundary conditions 47

7.4 Zoom on part of the geometry mesh. 48

7.5 Wall shear stress in 1 phase flow 52

7.6 Gas Phase Graph in the symmetrical 2D pipe with air injection of 0.1 m/s 53

7.7 Gas Phase Graph in the symmetrical 2D pipe with air injection of 0.1 m/s 53

7.8 Shear Stress distribution into the membrane 54

7.9 Shear stress profile for an air injection 1 m/s 55

8.1 Flux Decline comparison between 1 phase flow and 2 phase flow with air injection at 0.1 m/s 58

8.2 Flux Decline comparison between 1 phase flow and 2 phase flow with air injection at 1 m/s 59

8.3 Flux Decline comparison between 1 phase flow and 2 phase flow with air injection at 4 m/s 60

9.1 Particle Size distribution for oil droplets 62

Chapter 1

Introduction

Produced Water (PW) is a byproduct obtained during oil and gas extraction processes in both onshore and offshore industries. Water gets trapped together with oil and gas, inside porous rock formation between layers of cap rock sealed until the extraction.
The ratio between produced water to oil (WOR) or produced water to gas (WGR) is usually in the range between 0 and more than 50.[1] In a global average, the value of WOR is around 4 [2], while WGR is usually even bigger. These ratios are very likely to increase in the following years: produced water is, in fact, injected into the wells to sustain the pressure and increase the well extraction when the oil and gas production from a well starts to decrease.
Water coming out with the oil usually contains large amount of heavy metals, chemical compounds added during the extraction, dissolved and dispersed oil compounds and radionuclide. They could have a very high impact on the environment if released without any pre-treatment.
In order to avoid this, environmental legislation is becoming more and more demanding on the quality of disposal water, and even if there is not a common international regulation all the countries are starting to become more rigid about the argument. United States Environmental Protection Agency (USEPA) set the daily maximum limit for dispersed Oil and grease is 42 mg/L and the monthly average limit is 29 mg/L. Australian laws require a quality of waste water with

less than 30mg/L of oil and grease. China prescribed an average limit of 10 mg/L, while the Marine Environment of the North-East Atlantic (OSPAR Convention) has annual limit of discharge into the sea of 30 mg of dispersed oil per liter of produced water .[1]
In this scenario it is easy to imagine that the developing of technologies for oil/water separation becomes essential. These technologies needs to have high performances on the produced water quality but also be suitable for the oil production under the aspects of space required, without affecting the continuity of the operations.
Among the different technologies used for produced water, one is showing interesting characteristics, high efficiency and big margin of improvement: the membrane filtration.
Membrane filtration (Microfiltration, Ultrafiltration and Nanofiltration) can achieve a rejection of particle size up to 0.01 μm, which is one of the best performance among all the technologies as Table 1 shows.

Oil Removal Technology	**Minimum size of particles removed (microns)**
API gravity separator	150
Corrugated plate separator	40
Induced gas floatation (no flocculants)	25
Induced gas floatation (with flocculants)	$3-5$
Hydroclone	$10-15$
Mesh coalescer	5
Media filter	5
Centrifuge	2
Membrane filter	0.01

Table 1.1: Technologies compared on minimum particle size rejection

This technology allows continue operations on an incoming flow and, moreover, no settling time is required to obtain produced water, which is a big advantage for this kind of field.
The space and energy needed for this technology are very small and make it suitable for the transport on different locations. Also, a single membrane, can have a

lifetime up to 10 years, which is anyway less than the average of other technologies but a simple membrane replacement can restore the whole setup which is not possible for other technologies.[3]
Based on the particle size to reject, it is possible to use different membrane (micro/ultra or nano filtration) making this technology valid for a high range of different applications.
The main disadvantages of membrane filtration is the deposition of particles on the membrane (fouling) which affect the performances (permeate flux) and requires periodically cleaning operations in order to restore (or partially restore) their native efficiency.
This thesis will focus on the best operation conditions to limit these disadvantages.
In chapter 3 an overview of the membrane filtration will be provided, explaining how the filtration happens, the different kind of filtration existing, how they are used into a train and a presentation of the fouling problem with the factors influencing it.
Chapter 4 will give an overview of a two-phase flow characteristic with water and air injection, highlighting the benefits that could bring to the filtration process (becoming so a three-phase flow including the particles).
Chapter 5 will introduce a fouling model based on the shear rate, for crossflow filtration.
In chapter 6 the experiments, the setup and their aim will be introduced. The data obtained will be then used together with CFD simulations to obtain results from the models. Model introduced before will be eventually validated from the results.
Chapter 7 will use some boundary conditions from the experiments to simulate in CFD a two-phase flow (air-water without particles) which is not possible with the current setup used in the experiments. The data will also be stored to be used in the models to check eventual enhancement with use of air injection into the feed.
In chapter 8 results will be presented, joining the simulations results with a build-in Matlab script representing the mathematical-physical model for the membrane.
Last chapter will give conclusions of the following study.

Chapter 2

Problem formulations

The following work will include a study of a membrane cross-flow filtration, giving an overview of the physics phenomena behind the cross-flow process and fouling. These background studies will be applied to experiments in order to study the best operation parameters to achieve high performances out of this kind of filtration. CFD together with Matlab simulations will try to evaluate the best conditions for this technology simulating air injection into the feed and the consequences on the fouling.

The first step will be the creation of a Computational Fluyd Dynamic model which eventually will respond with accuracy to experiments with just pure water. The experimental setup will be composed by a filtration unit with a monolithic silicon carbide membrane monotube.

An existing analytical model to describe the permeate flux decline in cross-flow filtration with fouling will be used and should be experimentally validated. The support of computational fluid dynamic simulations will provide inner flow parameters.

A good model is very important in order to study the produced water process. The model correlates different factors and boundary conditions of this technology through scientific/physic approach, giving the possibility of predicting output parameters of interest like the steady state flux, the permeate flux and time to reach it. With a good model and good predictions, it is possible to study the best

boundary conditions to improve the overall system. Once validated the model, new simulations with a two-phase flow will be processed (pure water with injection of air) for different water/air ratios evaluated through a flow pattern calculation. Values obtained from these simulations will be used into the analytical model to obtain the evaluate the performances, using as evaluation criteria both the permeate flow and the reduction of fouling effects.
This study will focus mainly on the idea that the fouling can be heavily influenced by the wall shear stress, which can be increased through gas injection and in which range can be effective. It will eventually provide indications on how to find the best operating conditions to reduce the fouling, extend the time between the cleaning operations with a lower energy waste.

2.1 Delimitation

This thesis will mainly focus on a two-phase flow (air-water) studying the indirect effect of its parameters on the three-phase flow (air-water-fouling particles).
The experimental setup will be used with water and fouling particles without any gas-injection and compared with the model. Gas injection will be then simulated into CFD.
The three-phase model will not be then experimentally validated. It is possible, anyway, to assume that a good correspondence between the experimental fouling flux decline and the modelled one, could give a good correspondence also on the flux decline with gas injection into the feed.
The study of the fouling will be performed in a qualitative way, keeping in consideration parameters that are considered related to the phenomena without a simulation of the exact physics of the particles accumulation on the membrane.
The problem will be limited to the MF, in order to have more accurate data with our experimental setup.
The experimental membrane setup provided by the university will be used for the first time in this thesis's experiments, so assembling, testing and eventual corrections will be an actual part of this thesis work.

Chapter 3

Introduction to Membrane Filtration

Membrane filtration uses the concept of semi-permeable membrane. A semi-permeable membrane is a membrane which allows a partial passage of molecules or ions through diffusion. The properties of the membrane material together with the properties of the solute (pressure, concentration and temperature) defines the rate of rejection from the stream of water. The solute passing by a permeable material experiences a reduction in the concentrations of particles, due the particle retention in the membrane pores.

It is very important for the membrane materials to have a good resistance which means it is possible to push the pressure and temperature to high value without creating any damage to the membrane and have a good quality of filtration.

Filtration happen in two different zones: on surface where the particles with a larger diameter than the pore size get stuck, and in the depth where the the particles are trapped because of the tortuous path inside the material. Figure 3.1 provides an idea of what happens during the process. [3]

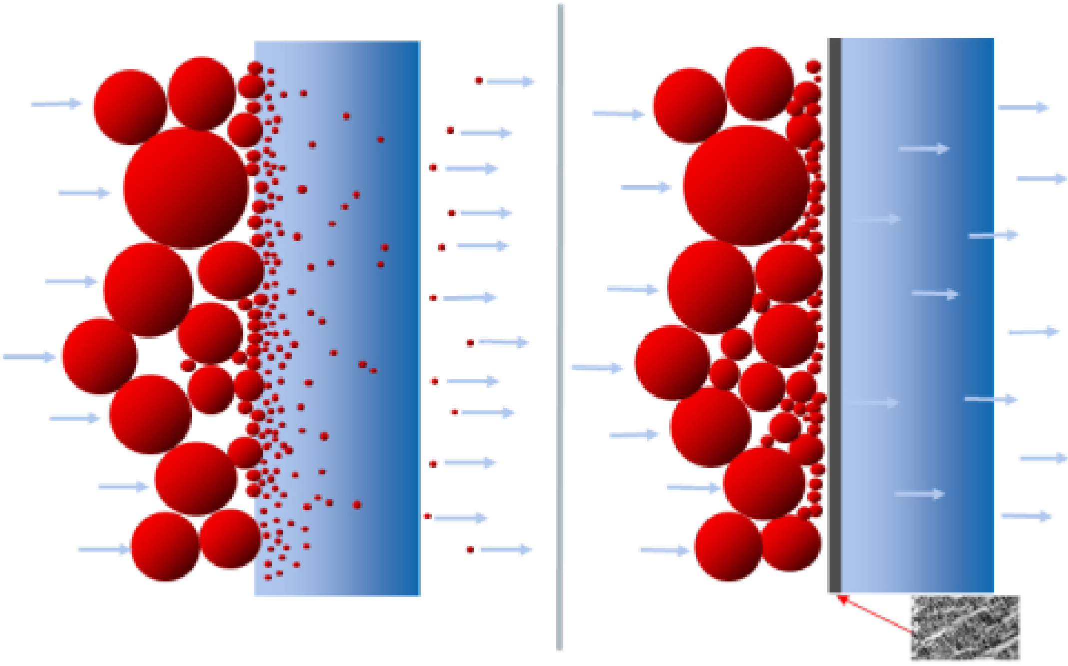

Figure 3.1: In the depth filtration particles accumulate inside the material (left), on the surface filtration (right) a cake layer creates on surface [4]

3.1 Membrane filtration processes

Based on the particle size processed there are 4 different types of membrane filtration.

- Micro Filtration
- Ultra Filtration
- Nano Filtration

Micro Filtration

Micro Filtration operates on particles with a range in the diameter size between 0.03 μm and 10 μm. It is used with a relative small pressure (100 kPa to 400 kPa) and velocities in the order of 1-3 m/s.
It is widely used for removing large suspended particles or as pretreatments for

Nano Filtration and Reverse Osmosis. Impossibility or limited partial bacteria removal is one of the reasons for a confined use

Ultra Filtration

Pore size of Ultra Filtration membranes stays in a range between 0.002 to 0.1 μm, the operating conditions are between 200 to 700 kPa.

UF has a wider removal of bacteria and virus compared to the MF but it is not a barrier for them and moreover a complete removal of micro-biological species can be achieved.

Nano Filtration

Nano-filtration membranes have a pore size of about 0.001 μm and are used at a working pressure of about 600-1000 kPa. They are able to remove all viruses and bacteria together with alkalinity which can make water corrosive.

Overview of the particles rejection based on the type of filtration is illustrated in Figure 3.2

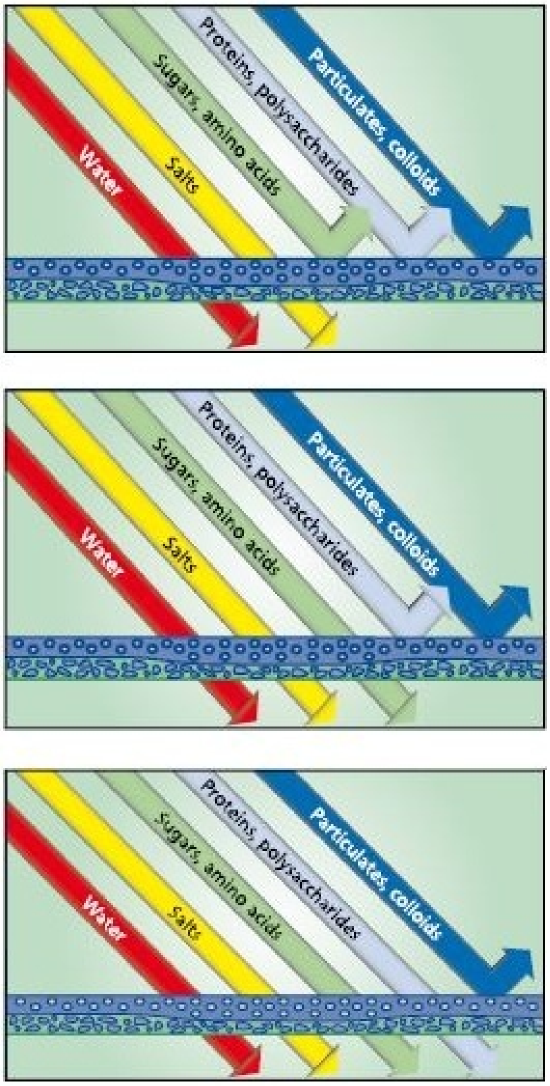

Figure 3.2: Particle retention for the different filtration processes. From the top to the bottom :NF, UF, MF

[5]

3.2 Crossflow vs Dead-end

Membrane filtration can occur in two different lay-out: Crossflow and Dead-end. Figure 3.3 shows the main differences in the flow directions. In the dead-end filtration, the feed and the permeate stream have the same direction. In this setup, there is no retenate flow because all the feed passes through the porous material converting into permeate flow. This kind of filtration can be used when the feed water contains a low level of foulants, since this method usually requires an high number of backwashes and membrane replacement, because of a cake layer formation.

In the Cross-flow filtration the feed stream is perpendicular to the permeate. The pressure gradient over the membrane affects the ratio between permeate flow and feed flow.

Compared with the dead-end, crossflow filtrations has a lower permeate flow but also less maintenance required (replacements of membranes and number of backwash). It is widely used also because it can be used in series inside a bigger setup where the retenate flow of a membrane is the feed of the next one.

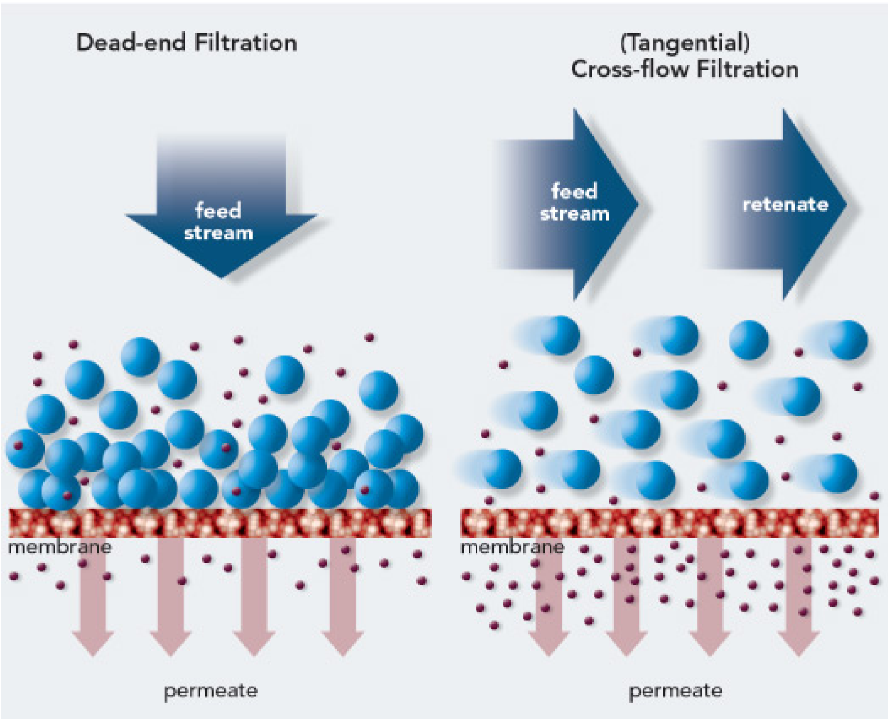

Figure 3.3: Example of dead-end filtration and crossflow filtration[6]

3.2.1 Cross-Flow

The following thesis will follow the study of a tubular crossflow membrane. A model will be introduced in Chapter 5 describing its characteristics.

3.3 Membrane Train

The membranes are used in series in order to reduce the retenate flow. The whole unit with multiple membranes in series is called "pressure vessel". Multiple pressure vessel can be used in parallel in order to increase the production and also avoiding a total stop of operations during the backwash cleaning.
It is common to use a so defined "Pyramid structure", in which different stages of vessels are used. Usually the ratio between two stages is 2:1. As it is possible to observe in Figure 3.4 different vessels are used for a first stage parallel filtration. The permeate is then accumulated all together while the feed go under a new filtration stage with half of the number of vessels of the previous stage.
[7]

3.4 Fouling

One of the biggest limitation to a wider use of the membrane technology in PW is the phenomena of the fouling which affects the filtration performances and makes regular membrane cleanings required.
Fouling is the accumulation of particles on the membrane which obstructing partially or completely the pores decreases the permeate flux and also affect the quality of water. There are two different kind of fouling: reversible and irreversible.
Reversible fouling can be removed through back-washing but, if the process of filtration continues without any backwash for a long period, can become irreversible.

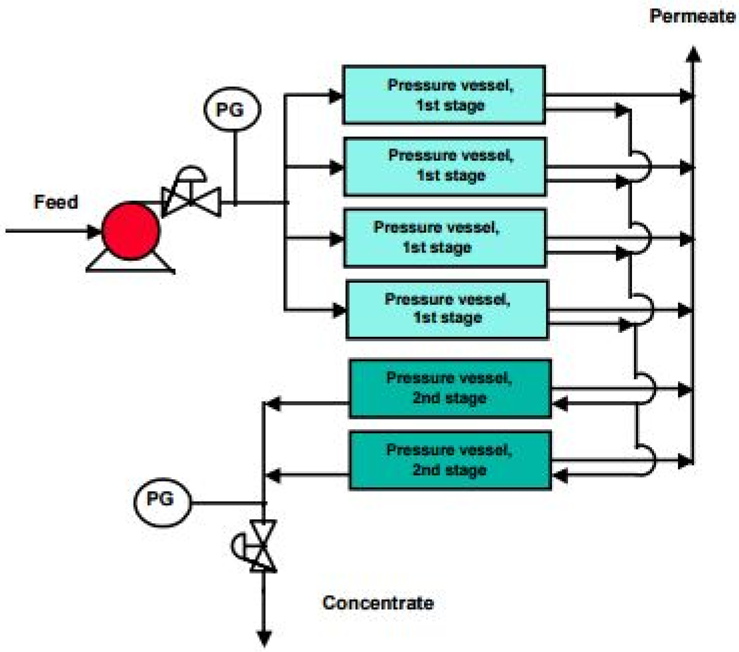

Figure 3.4: A common application of membranes, combining both membranes in series (vessel) and in parallel.[7]

This means the fouling layer cannot be removed and be restored to its original condition.
There are four kind of fouling:

- Inorganic fouling/scaling
- Particle/colloidal fouling
- Microbial/biological fouling
- Organic fouling

The permeate flux decrease is caused by an increase in the membrane resistance due to the pores occlusion and cake layer formation on membrane surface.
The membrane fouling can be divided in three phases.
In the beginning the permeate flux is maximum, because the membrane is clean and its pore free. There is soon a fast decrease of the flux due to quick blocking of membrane pores. The dimension of the particles in the retenate flux has a big importance in the kind of blocking effect on the membrane and the development of the fouling, as it is possible to observe in the figure 3.5.
The second phase is a new decline in the flux due to the formation of a cake layer,

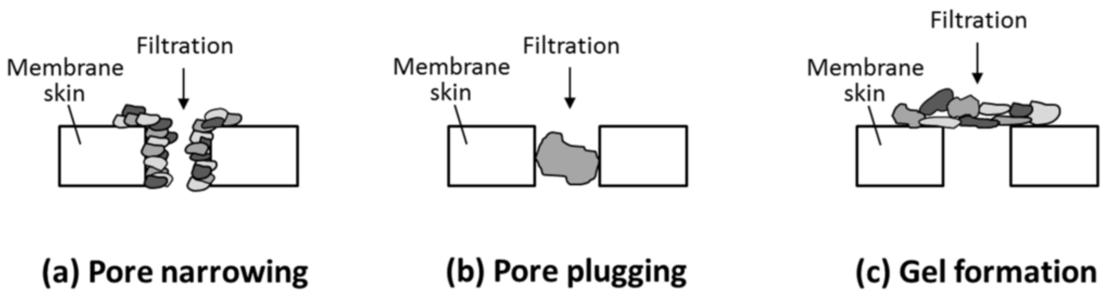

Figure 3.5: Three different cases in fouling: a) Membrane pore diameter bigger than particle diameter b) Membrane pore diameter approximately the same size as particle diameter c) particle diameter bigger than membrane pore size [8]

which grow fast in thickness and increases the membrane resistance.
In the very last phase the flux becomes pretty much constant stabilizing at its

minimum amount of permeate flow. A plot of the flux decline as function of time is provided in figure 3.6[9]

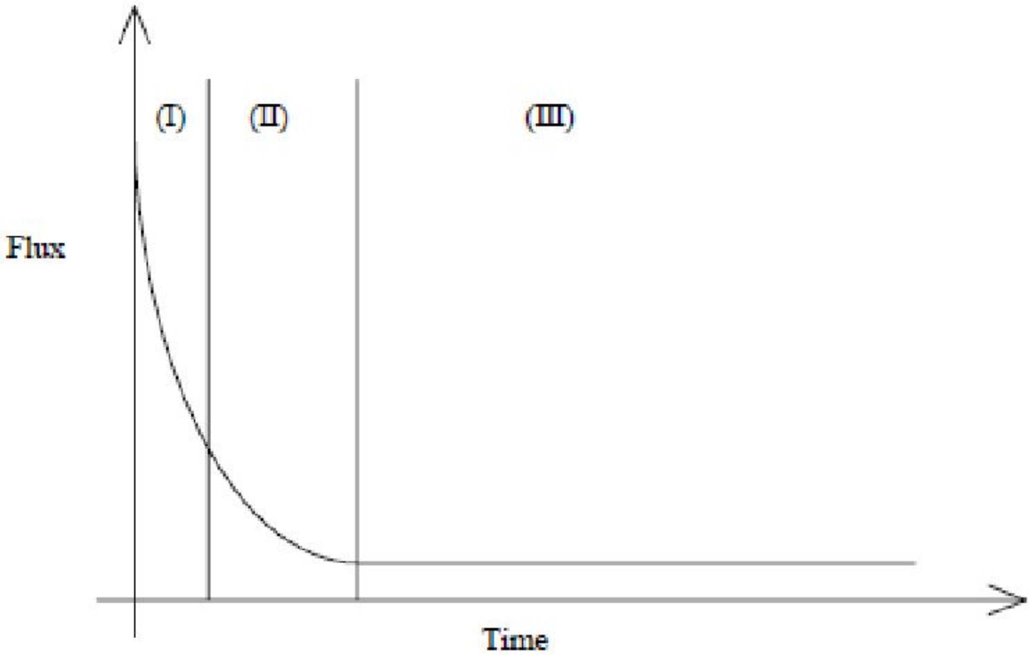

Figure 3.6: Three phases of the flux decline due to the fouling [9]

3.4.1 Backflush

The backflush (or backwash) is a method used to restore the performances of the membrane when the flux declines due to the particle deposition on the membrane. Injecting water at high pressure in the opposite direction of permeate flow, the particles are expelled from the membranes pores and accumulate into the waste stream. This operation can not restore the membrane totally, due to the irreversible fouling . The backflush performances recover are less effective with the dead end filtration compared with the crossflow one. The figure 3.7 shows a plot of the flux as function of time and backflush operations.[3]

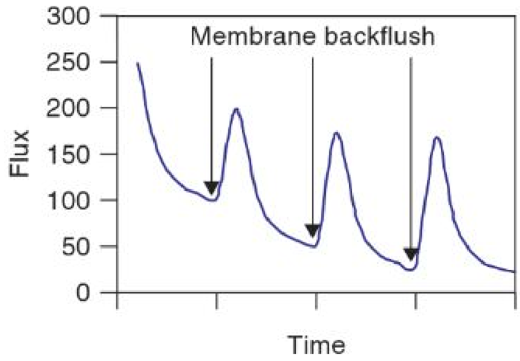

Figure 3.7: Permeate Flux vs Time and effects of backflush operations [3]

3.4.2 Fouling Model: Darcy Law and Important Parameters

A porous medium is composed by a solid part, also called solid matrix which contains pores in its inside. The pores are interconnected in order to make the volume permeable. In order to describe the deposition of fouling particles on the membrane, it is important to define the parameters involved into the model.

Based on the turbulence it is possible to define different regions of behaviour for a flow in a porous media. The first region is called Pre-Darcy flow, it happens just for very slow flows and its actual existence is still in discussion. The second region is Darcy flow and is applicable for laminar flows, with Reynolds number in the range $10^{-5} < Re < 2.3$. The third region is a region of transition between laminar and turbulent called Forchheimer region. This flow happens $5 < Re < 80$. Last region is turbulence region and it is for flow with Reynolds number over 200. For the aim of the following thesis, and in general for all the membrane studies, the reference region for the porous media is the Darcy Region. Darcy region is described by the following law, called Darcy's law:

$$v = -\frac{kTMP}{\mu w} \tag{3.1}$$

k = Permeability [m^2]
μ = Viscosity [Pa s]
v = Permeate Flux [m/s]
TMP = Trans Membrane Pressure [Pa]
w = Membrane wall thickness [m]

v represents physically the velocity of the permeate flow in the porous media and is equal to the permeate flow Q_p divided by the filtration Area A.
In the Darcy region it is possible to make different assumptions to simplify the problem.

- Isotropic medium
- Constant Pressure gradient
- Constant density of the fluid
- Saturated porous medium

Trans Membrane Pressure

Trans Membrane Pressure is the pressure pressure difference acting on the membrane wall. It is the driving force of the permeate flow (which is the actual filtration) and is very important, parameter.
In order to describe this value it is possible to start from the Hagen-Poiseuille Law.

$$Q_{pipe}(x) = \frac{\pi r^4}{8\mu}\frac{\Delta p(x)}{w} = \frac{-\pi r^4}{8\mu}p'(x) \tag{3.2}$$

The permeate flow for the Darcy Law is expressed by equation 3.1. It can be then re-arranged in our case as:

$$Q_{permeate} = \frac{2\pi rk}{\eta}\frac{\Delta p(x)}{w} \tag{3.3}$$

Using both the continuity equation for the flow, and definition of derivative applied

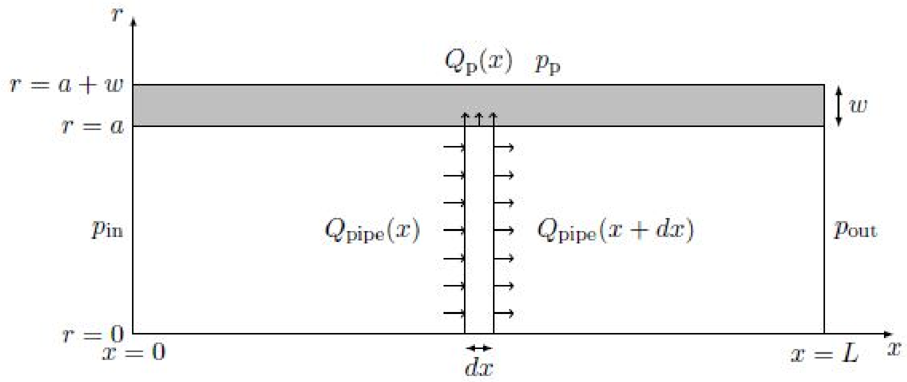

Figure 3.8: Illustration of a 2D flow through a porous media [10]

on the pressure $(p'(x) - p'(x+dx))/dx = p''(x)$ it is obtained:

$$p''(x) = \frac{1}{\lambda^2}\Delta p(x), \lambda = \sqrt{\frac{r^3 w}{16k}} \tag{3.4}$$

The solution of this differential equation considering $\Delta p = p(x) - p_p$, is:

$$p(x) - p_p = Ae^{\frac{x}{\lambda}} + Be^{\frac{-x}{\lambda}} \tag{3.5}$$

Adding boundaries conditions $p(L) = p_{out}$, $p(0) = p_{inl}$ $p_p = 0$, the solutions becomes:

$$p(x) = p_{inl} + \frac{x}{L}\left[p_{out} - pinl - \left(\frac{L}{\lambda}\right)^2\left(\frac{1}{3}p_{inl} + \frac{1}{6}p_{out}\right)\right] + \frac{1}{2}\left(\frac{x}{\lambda}\right)^2\left[p_{inl}\left(1 - \frac{1}{3}\frac{x}{L}\right) + \frac{1}{3}p_{out}\frac{3}{L}\right] \tag{3.6}$$

Since the coefficient $\frac{L}{\lambda}^2$ and so $\frac{x}{\lambda}^2$ <<1 , the pressure can be considered linear through the pipe. This means that the transmembrane pressure, the pressure difference between the porous wall is equal to:

$$TMP = \frac{p_{inl} + p_{out}}{2} - p_p \tag{3.7}$$

Where:

P_{inl} = feed pressure [bar]
P_{out} = retentate pressure [bar]
P_p = permeate pressure [bar]

The transmembrane pressure will be approximated with the previous formula in the following thesis.

Permeability

The permeability of a porous media is a parameter used to simplify the description of a flow inside these kind of materials, which have a very complex inner geometry. The porous field is described as continuum where the hydraulic resistance of the pores is considered as mean hydraulic resistance of the whole medium.
The permeability is function of three different values:

- Porosity
- Sphericity
- Tortuosity

Porosity is the ratio of the void volume on the total volume:

$$\phi = \frac{V_{void}}{V_{total}} \tag{3.8}$$

Sphericity is the ratio between the particle of porous media surface and volume.

$$S = \frac{A}{V_{total}} \tag{3.9}$$

For perfect spherical particle can be written:

$$S = \frac{6}{d_m} \tag{3.10}$$

Last value is the tortuosity and is the ratio between the shortest path between two points in the medium (usually inlet and outlet) and the actual distance that a flow should do.

$$\tau = \left(\frac{L}{X}\right) \tag{3.11}$$

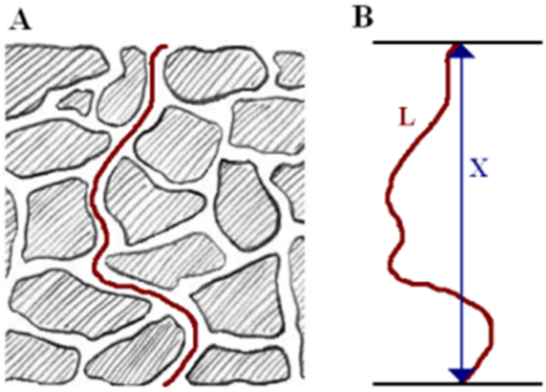

Figure 3.9: A)Overview of a porous media in a section parallel to the flow B) Shortest path(X) and the actual flow path (L) [11]

Permeability is expressed in Kozeny-Carman equation as:

$$k = \frac{\phi^3}{S^2 kc(1-\phi^2)} \tag{3.12}$$

kc is a value called Kozeny-Carman constant. It is inverse proportionally to the tortuosity and experiments in different literature report good matching using a value of 5.[12][13][14]

The previous equation becomes then equal to:

$$k = \frac{d_m^2 \phi^3}{180(1-\phi^2)} \tag{3.13}$$

The value obtained from the equation is anyway just an approximation and needs to be experimentally obtained for a better accuracy.
In order to obtain it experimentally it is possible to apply Laplace equation to a 2D flow (Dead-End would be 1D, while crossflow is 2D).

Combining the continuity equation for incompressible fluid $\Delta v = 0$ with the Darcy law previously presented, it is obtained a Laplace equation to describe the pressure distribution on a porous media.

$$\Delta^2 p = 0 \tag{3.14}$$

Considering the Dirchlet conditions, with the pressure inlet and outlet at the inner and outside radius of an annulus (r_{in} and r_{out}) (the cross section of the Sic monotube is the 2D problem analysed) the pressure is described by the following equation:

$$p(r) = \frac{p_1 - p_2}{ln\frac{r_{in}}{r_{out}}} ln\frac{r}{r_{in}} + p_1 \tag{3.15}$$

Using the Darcy Equation and integrating the previous equation it is possible to obtain the Permeate flux in a 2D flow.

$$Q_p = \frac{2\pi L k \Delta P}{\eta \ln(1 + \frac{w}{r_i n}}) \tag{3.16}$$

Rearranging it:

$$k = \frac{Q_p}{TMP} \frac{\eta \ln(1 + \frac{w}{r_{in}})}{2\pi L} \tag{3.17}$$

3.4.3 Fouling Model

So far the equations presented were valid for a fluid passing through a porous media, with a constant value of the permeability.
When the effects of the fouling needs to be accounted the value of the permeability decrease with the time.
Usually when dealing with fouling it is more common to use the value hydraulic resistance, which is a sort of permeability averaged for the length of the medium.

$$\frac{-k}{w} = R \tag{3.18}$$

The reason for this rearrangement is because the hydraulic resistance can be considered as the sum of two resistance in series: the clean membrane resistance R_m. This hydraulic resistance is used into Darcy Law to calculate the permeate flux , using the resistance in series with the membrane hydraulic resistance (R_m), and the hydraulic resistance of the cake formation R_c.

$$v = \frac{TMP}{\mu R_m + R_c} \tag{3.19}$$

Where:

$$R_c = rcm_d \tag{3.20}$$

rc = specific cake resistance [m/kg]
m_d = mass of the deposit per unit area [kg/m2]

The hydraulic resistance of the cake formation R_c can be considered as the sum of three different factors:

- R_{pl}: the polarization layer resistance
- R_{ad}: fouling resistance caused by particles adsorption
- R_f: fouling resistance, which can be divided in irreversible and reversible

R_{pl} can be easily recovered through an use of the membrane with deionized water at the same operating condition, R_{ad} has a very small contribute to the total fouling and can be approximately ignored also because it is independent from the permeate flux
As mentioned before the irreversible flux is the most problematic part which is caused by pore blocking, strong cake, gel and biofilm. The reversible fouling part is cyclic eliminated with backflush, while the irreversible can't be eliminated and in a long period can bring to very low performances. In order to obtain constant operating system conditions, the decrease in the performance must be compensated by a higher pressure gradient, which of course is an additional cost of money.
The highest concentration of particles reach the maximum after a very short period due to high flux, creating the three different resistances layers mentioned

(reversible, irreversible and particle concentration). The inner reversible fouling becomes more compact and increase its density and if not backflushed can become irreversible in a short period.

3.4.4 Influences on Fouling

Fouling can be influenced by different parameters, one is the choice of the membrane.
An important characteristic of the membrane for its ability to attract particles is the wettability. The wettability is a parameter that can be roughly observed by measuring the contact angle between a droplet of liquid and the membrane surface. The hydrophilic membranes have tendency to absorb water because of their tendencies to form hydrogen bonds with water, while hydrophobic (high wettablity) tend to reject water and are the most subject to fouling phenomena. This kind of membranes can still be used but a treatment to make their surface hydrophillic is suggested.
Another important factor is the temperature. At higher temperature the permeate flow increase, and this suggests a decrease of fouling phenomena. The data suggest that increasing from 20 to 40 an increase of 60% in the permeate flow is obtained. At low pressure the TMP has a high influence on the permeate flow, but over a certain limit the permeate flow will not increase. The same phenomena is not happening with just pure water. This is caused by gel formation of the polar particles at high pressure.
Among the most important physical parameters there are the crossflow velocity and the shear stress forces.
An efficient choice of cross-flow velocity can reduce the value of reversible fouling. This is very important for the performance and also because allows to reduce the backflush operations without any danger for irreversible fouling formation.
Crossflow effect has influence in the reduction of reversible fouling in the range from very small velocity (0.2 m/s) to middle high (3 m/s) velocity. Over a certain limit, called the critical crossflow velocity, an increase of the crossflow velocity does not bring any reduction of reversible fouling. [15]

The critical cross-flow speed, can change and is of course function of porosity, pore size, permeability of the membranes. In order to obtain the exact value for a specific membrane , experiments should be conducted.
In the figure 3.10 it is possible to observe a series of experiments conducted on a membrane with different crossflow velocities.

Shear stress acting on membrane due to the feed water avoids the collection

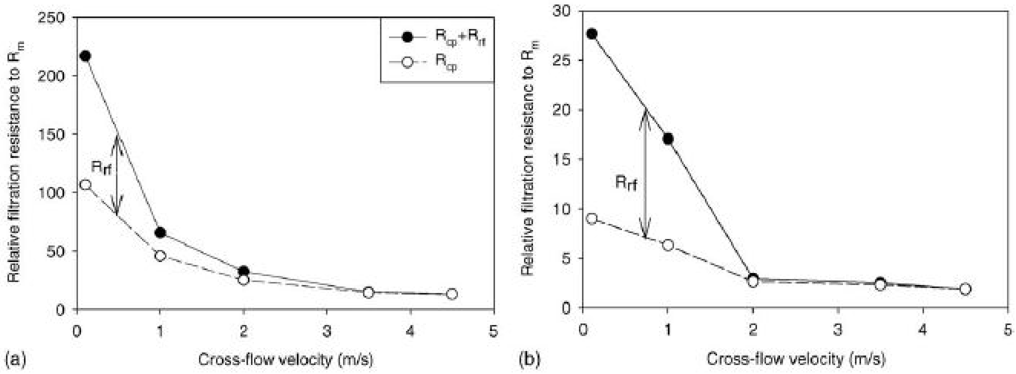

Figure 3.10: Filtration resistance by the formation of reversible fouling layer after 4 h of filtration at different cross-flow velocities: (a) MF and (b) UF. [15]

of reversible fouling on their surface. Different studies were conducted in order to check what kind of shear stress is the most efficient in the membrane fouling control. It is possible to distinguish 4 macro groups of shear-stress(Figure 3.11): [16]

- Continuous surface shear stress profile.
- Sustained peak surface shear stress profile.
- Low peak surface shear stress profile.
- High peak surface shear stress profile.

The continuous surface shear stress profile is a shear stress with an almost steady value with small magnitude of pressure. It can be compared to a single-phase with

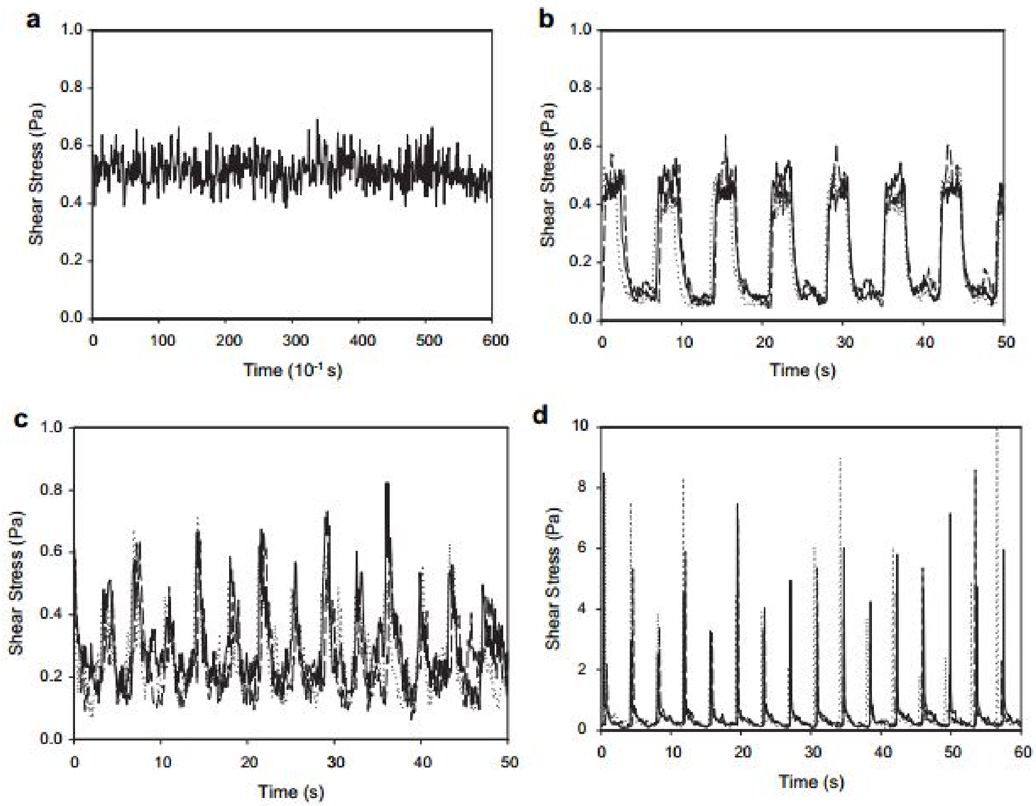

Figure 3.11: Pressure vs time graph for : a) Continuous surface shear stress profile. b) Sustained peak surface shear stress profile c) Low peak surface shear stress profile. d) High peak surface shear stress profile. [16]

no gas injected.

The Sustained peak surface shear stress profile is characterized by high stress long transients followed by sustained peak surface shear stress profile. The duration of this stress is higher then the low peak surface and high peak surface profile.

The low peak surface shear stress profile is similar to the one just described but with a very small settlement time of the stress peak.

The High peak surface shear stress profile has very high magnitude of shear stress in very short time, followed by sustained peak.

High peak surface shear stress and sustained peak surface were the most effective in the fouling control, low peak surface shear stress and continuous surface shear stress had the poorest results in the fouling prevention. A transient shear stress is

usually considered the best way to reduce the fouling.
From some of these studies it is suggested that a minimum of energy is required before the transport of particles from membrane can occur, as it is showed by the best performances of the high peak compared to the low peak profile.
Frequency is also a parameter to consider, but so far it was hard to define a correlation with the fouling, but connections have been observed. The three main parameters are: time-averaged shear stress, standard deviation of shear stress, and the ratio of averaged shear induced by two-phase flow conditions to the averaged shear stress induced by single-phase flow.[16]. Shear Stress will be the main focus in this thesis evaluation of the fouling phenomena.

3.4.5 Pretreatments to fouling

There are different treatments that is possible to execute in order to decrease the fouling into a membrane and increment its lifetime. One way to achieve this is to pre-treat the feed water to control colloidal, organic and biological fouling.
One of the most widely used technique is the coagulation. Coagulation uses different chemicals to increase the size of the particles before the filtration. This allows to decrease the reversible fouling but this method is ineffective against irreversible fouling since this increase of size does not include the very small particle which still accumulate creating irreversible fouling.
Flocculation is a similar process which uses flocculants to help settling of suspended particles making them bigger, and hence increase the permeate flux.
Magnetic Ion Exchange (MIEX) uses polymer beads in order to adsorb particle with a positive or negative charge. The dissolved organic carbon (DOC) is mainly composed by polar substances, so this method has high efficiency on these kind of particles.

3.4.6 Membrane Cleaning

Membranes start to decrease their performances with the time due to fouling effect. The permeate flux decrease and has lower quality than a permeate flux obtained with a clean membrane. Cleaning operations are required to restore the efficiency of the filtration. Fouling can be removed by backwashing or chemical backwashing. It is possible to have two kind of operations: CIP (cleaning in place) operation, which use the same setup without any remove of the membrane, and off-line chemical cleaning.

Backwashing uses the permeate flow, in a reverse direction, in order to clean from the particles the membrane pores. Chemical Backwashing is used when standard flush or backwash is not enough to restore the membrane. Some chemicals to help the cleaning operations is added and is used in a loop for a short period to clean the membrane.

Different membranes reacts differently to the cleaning operations, in the following table it is possible to compare the effectiveness of different techniques.

Some particles such as calcium, magnesium and silica scaling can not be filtered

	Effects of Operating Strategy			
Type of Fouling	**Backwashing**	**Feed Chlorination**	**Feed Acidification**	**Chemical Cleaning**
Inorganic	-	-	++	++
Particulate	++	-	-	++
Microbial	+	++	+*	++
Organic	-	+	-	++

Table 3.1: Cleaning method effectiveness on fouling
[9]

through membrane, so acid wash is needed.

High temperature and hydrodynamic conditions that enhances a better contact surface between fouling and cleaning are very important.[9]

Chapter 4

Two Phase flow

[17]

4.1 Flow Patterns

In a two-phase flow with air and water, based on the different air and pipe direction , the flow could have several patterns. Based on the shear stress profiles presented in Chapter 3, it was experimentally found that a not constant high shear stress profile is the best way to avoid the fouling deposition. For this reason a discontinuous flow will probably be the best option.
In a vertical pipe it is possible to find four different patterns.

- Bubbly flow: the bubbles are small and approximately of an uniform size
- Plug flow or slug flow: the gas forms large bullet shape bubbles and small bubbles around it.
- Churn flow: The liquid near the wall pulses up and down and is very unstable flow
- Annular flow: the liquid flow forms an annular with some some droplets in the central core were the air is.

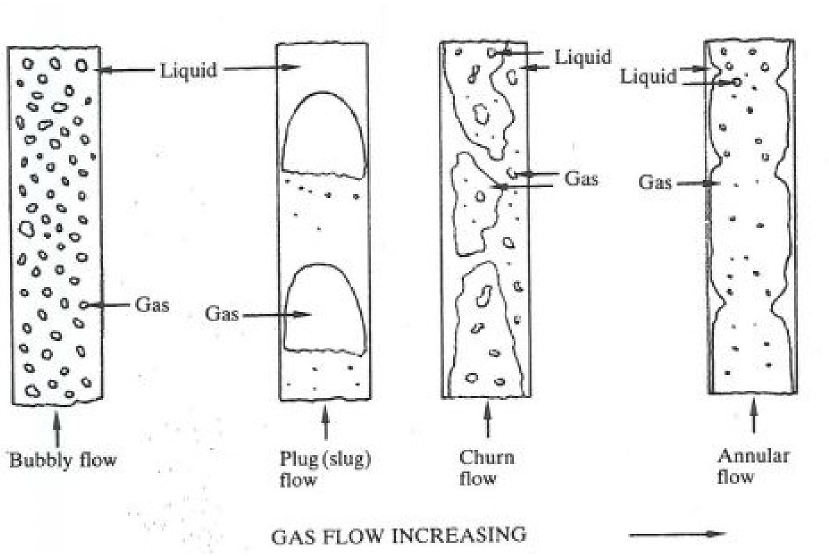

Figure 4.1: Different flow patterns for two-phase flow in an vertical pipe

In a horizontal pipe different patterns can be established. They are:

- Bubbly flow: gas tends to flow on the top part of the pipe in small bubbles.
- Plug flow: similar to vertical plugs but influenced by the gravity, the bubble with bullet shape stays in the upper part of the pipe.
- Stratified flow: The two phase separation is really smooth and regular. This pattern is actually not very common.
- Wavy flow: Similar to the stratified flow but with an interface less clear.
- Slug flow: As in the wavy flow the distinction between gas phase and liquid phase is clear, but the waves are so strong that can touch the top part of the pipe.
- Annular flow: The liquid film form an annular shape inside the pipe , while the gas stays in the core part of the pipe with some small liquid droplets transported by the gas flow .

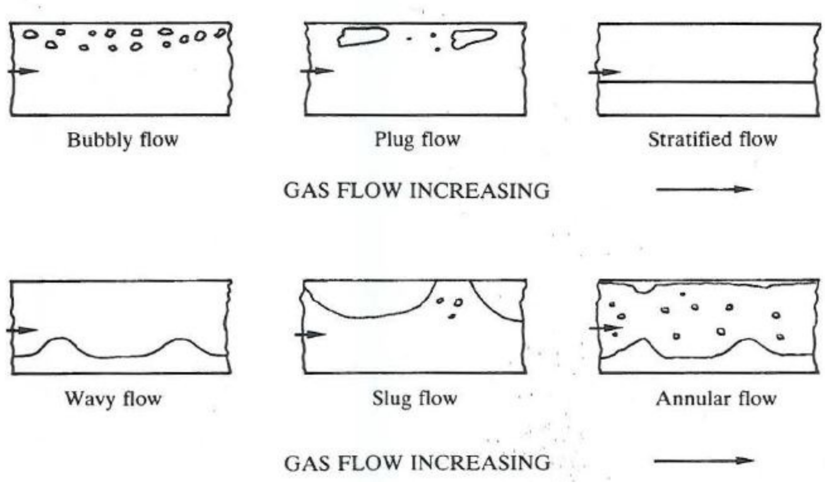

Figure 4.2: Different flow patterns for two-phase flow in an horizontal pipe

Hewitt and Roberts created a map of both the horizontal and vertical pipe to define the two-phase flow pattern based on the mass flux of gas and liquid, density and superficial tension of the phases.

$$G_g = massfluxofgas = \frac{gasmassflowrate}{tubecrosssectionalare} = \frac{kg}{m^2 s} \tag{4.1}$$

$$G_l = massfluxofliquid = \frac{liquidmassflowrate}{pipecrosssectionalarea} = \frac{kg}{m^2 s} \tag{4.2}$$

From empirical and technical limit data, we can assume that our flow will lie in the slug flow for vertical pipe. This pattern being discontinuous can be considered actually very good to avoid fouling for the reasons previously mentioned. The best empirical conditions for the shear stress have been proven to be, in fact, high shear stress with about 1 Hz frequency [18]. Here, every bullet shape bubble (with a liquid film around) is followed by a liquid region which will eventually have a lower shear stress on the wall, giving both a high frequency and high shear stress.

Studies on the patterns in two-phase flow are still ongoing and are not yet completely understood.

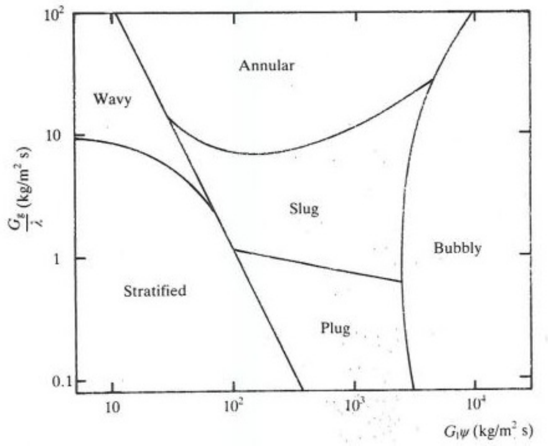

Figure 4.3: Map for horizontal two phase flow patterns
$\lambda = \frac{\rho_g}{\rho_a ir}\frac{\rho_l}{\rho_{water}}^{1/2}$ and $\psi = \frac{\sigma_{air-wat}}{\sigma}\left(\frac{\mu_l}{\mu_{water}}\left[\frac{\rho_{water}}{\rho_l}\right]^2\right)^{1/3}$
[17]

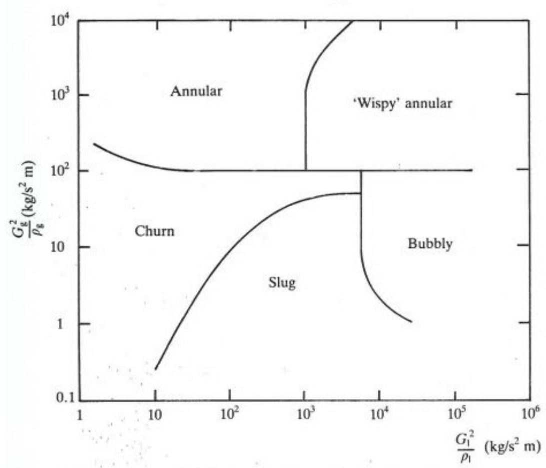

Figure 4.4: Map for vertical two phase flow patterns [17]

4.2 Benefits

Two phase-flow should cause an increase in the wall shear stress. This could bring different benefits to the performances of a membrane.

Mass Transfer

The mass transfer coefficient can also be related to the shear stress, following Leveque formulation, it can be expressed as:

$$k = 1.62\left(\frac{D^2\gamma}{L}\right)^{1/3} \tag{4.3}$$

D represents the diffusivity coefficient, L is the membrane length and γ is the shear rate.

Crossflow velocity

High gas sparging can increase the crossflow velocity which has an effect on the filtration resistance, and so the permeate flow, as it is possible to see in figure 3.10.

Particle deposition model

The high shear stress avoids the deposition of the particles, a model will be presented in the following chapter.

Chapter 5

Model Description

The model which will be used has been studied from Lianfa Song and published in the article "Flux decline in crossflow microfiltration and ultrafiltration: mechanisms and modeling of membrane fouling". In the paper, membrane fouling is studied as a transient process from a non equilibrium state (clean membrane) to a steady state equilibrium (minimum permeate flux). The particle deposition on the membrane and the consequent cake formation is the passage from transient to equilibrium, which will be achieved when the cake formation thickness reaches its maximum over all the membrane starting from the feed inlet.
The whole fouling process starts just if the TMP is over a certain value called critical pressure.
The model is studied divided in two main parts: the study of a dead-end filtration for the non-equilibrium part (A dead end filtration can be considered as an infinite length crossflow) and a steady state part, which can be combined to describe the whole process.
The model uses a mass balance to calculate the deposition of the particles on the membrane.

$$\delta(t) = \frac{1}{c_g} \int_0^t v c_0 dt \tag{5.1}$$

Where:

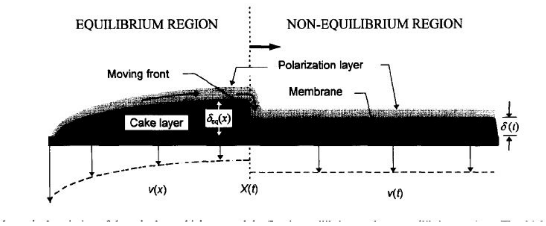

Figure 5.1: Front of equilibrium in a finite tubular crossflow representation [19]

c_g = volumetric cake concentration
c_0 = feed volumetric concentration
v = permeate flux
δ = cake thickness

This can be used together with the Darcy law and be rearranged as:

$$v(t) = \frac{\Delta P - \Delta P_c}{R_m + rc\delta(t)} \tag{5.2}$$

rc is the specific cake resistance.

The front of equilibrium (maximum thickness of the cake formation) will move in the same direction of the flow as Figure 5.1 shows, and with the integral method the flux can be estimated as:

$$v_{eq} = \left(\frac{2}{3}\right)\left(\frac{D^2\gamma}{x}\right)\left(\frac{c_g}{c_0} - 1\right)^{1/3} \tag{5.3}$$

D is the particle diffusion coefficient. γ is the shear rate, and x is the distance from the entrance of the section and equilibrium point.
With another mass balance is possible to track the equilibrium front and obtain and combining them all is possible to obtain the final equations averaging the flux over the channel and distinguishing two cases: before the steady state time and after.

$$V(t) = \begin{cases} \frac{1}{L}\left[\int_0^{X(t)} v(eq)dx + (L - X(t))v(t)\right] & \text{when } t < t_{ss} \\ 1.31\left(\frac{D^2\gamma}{L}\right)^{1/3}\left(\frac{c_g}{c_0} - 1\right)^{1/3} & \text{when } t > t_{ss} \end{cases} \tag{5.4}$$

Where:

$$\begin{aligned}
\mathrm{X(t)} &= 4.81(D^2\gamma)\frac{c_0}{c_g}^{1/2}\left(\frac{r_c t}{\Delta P - \Delta P_c}\right)^{3/2} \\
\mathrm{t}_{ss} &= 0.351\left(\frac{L}{D^2\gamma}\right)^{2/3}\left[\left(\frac{c_g}{c_0}\right)^{1/3}\left(\frac{\Delta P - \Delta P_c}{r_c}\right)\right]
\end{aligned}$$

A Matlab script was personally created in order to use this model and easily change the input parameters. It is presented in Appendix B.

Chapter 6

Experiments

6.1 Porosity

As previously mentioned, the porosity of the material is an important parameter in a Darcy Flow Region. For this reason experiments in order to obtain the value of it were performed.
The whole membrane was firstly weighted completely dry, and its weight was 24.85 g.
In order to check the volume of void inside the material, the membrane was immersed in water for 2 days so that liquid could fulfill all the void space.
The membrane was scaled after this operation and its weight was approximately 31.22 grams.
Considering the density of water at 20° is 1000 kg/m^3, it is possible to obtain the volume of the void.
$V = m/\rho$
V is the volume, m is the mass (in this case the mass difference between dry and wet) and the density is

$$V_{void} = \frac{(30.83 - 24.85)10^{-3}kg}{1000kg/m^3} = 0.00000597m^3 = 5970mm^3 \tag{6.1}$$

The total volume of the geometry is instead equal to:

$$V = (\pi R_e^2 - \pi R_i)L = \pi 5^2 - \pi 3^2 250 = 12566 mm^3 \tag{6.2}$$

$$\phi = \frac{V_{void}}{V_{total}} = \frac{5970}{12566} = 0.46 \tag{6.3}$$

The value provided by Liqtech is 43.6%. The difference could be due to drops retained inside the channels during the weigh operation.

6.2 Permeability and Membrane Clean Resistance

Cross-flow experiments were carried out in the monotubes membrane in order to correlate the Permeate flow and the Trans Membrane Pressure through the permeability parameter. In order to achieve the best results in the experiment was used distilled water with a constant temperature of 20 Celsius degree, and through the valves on the outlet were closed in order to obtain a dead-end setup.
The equation 3.16 , repeated here, show the dependence of the permeate flow on the pressure, viscosity (function of temperature), geometry and permeability.

$$Q_p = \frac{2\pi L k TMP}{\eta \ln(1 + \frac{w}{r_i n})} \tag{6.4}$$

The parameter of interest is the permeability, for this reason measurements were taken at different TMP, plotting the relatives permeate flux obtained.
Through the polyfit function of Matlab, the points obtained fitted in a linear equation, with a constant slope, as it is possible to see in the graph. The slope of the curve was called a. And from the slope it was possible to obtain the value of the permeability manipulating the equation 3.16.

$$k = \frac{a\eta \ln(1 + \frac{w}{r_{in}})}{2\pi L} \tag{6.5}$$

Inserting the information on the geometry of the monotube, it is possible to obtain the experimental value of permeability, which is:
k=1.7243e-15 m^2
From Carman equation (Equation 3.13), assuming the particle diameter equal to

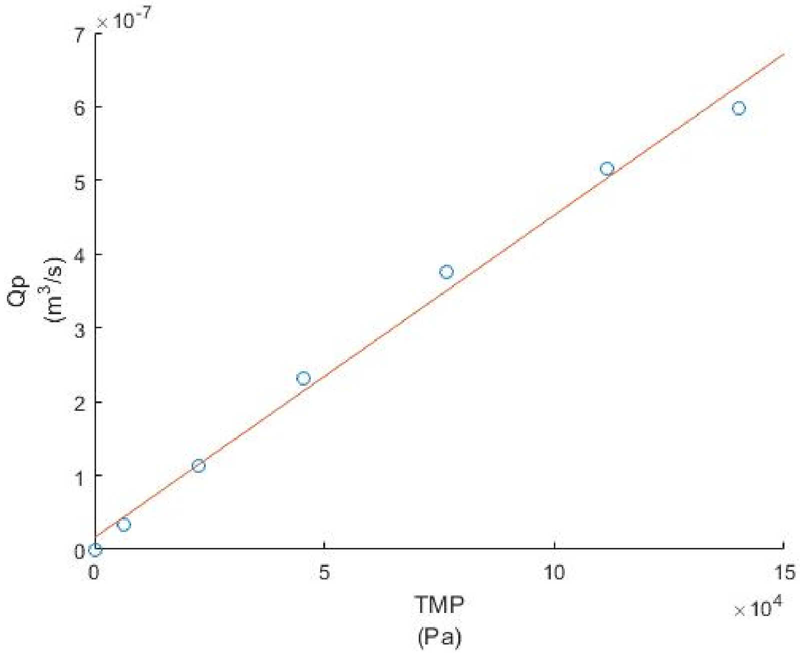

Figure 6.1: TMP vs Permeate Flux

the porous size, and using the porosity obtained in the previous section k should be equal to 6.3480e-11. This value is based on the hypothesis of perfect spherical particle, the pore size equal to porous media particle diameter. As mentioned before, the experimental value is more accurate.

Rearranging as function of Hydraulic Resistance using equation 3.18
Rm=1.45e12 $1/m$
It is also possible to check if the assumption of Darcy Region is correct: Reynolds number is equal to:

$$Re = \frac{vD}{\nu} \tag{6.6}$$

D is the hydraulic diameter which could be assumed equal to the pore size (0.1 μm), v is the maximum velocity of the fluid compared to the medium (it will be assumed Q/A_m), and ν is the kinematic viscosity which is equal to 1.00410^{-6}.

$Re \approx 1.510^{-5}$
This value lies in the Darcy Region.

6.3 Produced Water in Crossflow SiC membrane

In order to validate the model presented into the previous section, experiments were required. The experimental setup was recently acquired by university and part of the work of this thesis consisted into the partial assemblage of it, find the best solution to obtain the desired conditions for the experiments. Different difficulties were experienced in order to obtain the requirements since it was never used before.

6.3.1 Setup

In order to validate the fouling model an experimental setup built by Liqtech was used. LabBrain is a small setup in which it is possible to insert into its core a silicon carbide monotube membrane with a diameter of 10 mm, a wall thickness of 2.5 mm and 250mm length.
The membrane is housed inside a pipe and sealed on both the side with an O-ring. Two clamps allows to remove easily the membrane and change it.

Figure 6.2: Membrane and membrane housing

The setup is equipped with a feed pump which allows recirculation loop. It is possible to set the speed of the pump in order to have different feed/inlet conditions. To regenerate the membrane performance it is possible to use BackFlush

mode, which will clean the membrane from the fouling particles.
In the setup there are several transmitters and indicators which measures the flow and the pressure at different sections. There is a flow-meter at feed, while the permeate is obtained checking the weight of the permeate flux in a sample period (3 minutes) and reporting it into the SI units for flow through the density. The scale used has a precision of ± 0.005 g. The retenate (outlet) flow can be obtained through a mass balance. The pressure indicators read feed, permeate and retenate sections .

The figure 6.3 shows the diagram of the setup used. The components are listed

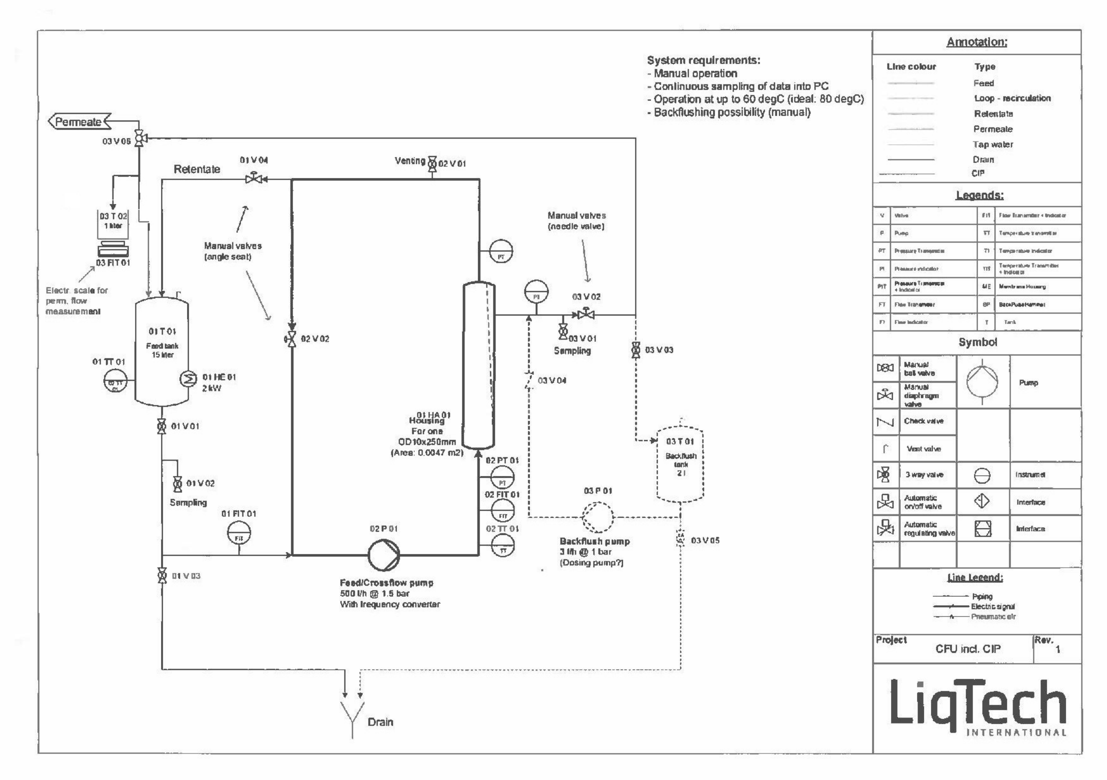

Figure 6.3: Setup Diagram for the experiment

in tables 6.1 6.2.

Instrument List				
Displayed Text	Description	Range	Manufacturer	Model
01 FIT 01	Feed flow transmitter	0.01 – 1.2 m^3/h	Siemens	MAG 5000
02 FIT 01	Crossflow flow transmitter	0.01 – 1.2 m^3/h	Siemens	MAG5000
01 TT 01	System temperature transmitter	0 – 100 °	Siemens	PT100
01 PT 01	Feed pressure transmitter	0 – 6 bar	BD Sensors	P200
02 PT 01	Permeate pressure transmitter	0 – 6 bar	BD Sensors	P200
03 PT 01	Retenate pressure transmitter	0 – 6 bar	BD Sensors	P-200

Table 6.1: Instrument List of the Setup

Equipment List			
Displayed Text	Description	Manufacturer	Model
01 P 01	Feed Pump	Grundfos	MDGRISC
03 T 01	Backflush tank	MT Membrane Tec	

Table 6.2: Equipment List

6.3.2 Produced Water Experiment Description

The tank was filled with 3 liters of distilled water, and 30mL of latex particles with a mean diameter of 0.1 μm. The volumetric concentration of the feed water obtained in this solution was 1% .

The water level inside the tank was enough to guarantee a constant water flux inside the pump, and avoid to run it dry damaging it.
Water was pumped inside the membrane. The permeate cross-flow went into the feed tank in order to keep the feed concentration constant. In order to calculate the permeate flow a sampling valve was opened when needed.

A sample of the fouling particles produced by Sigma was tested to check their mean diameter distribution. The standard deviation was very narrow and the mean particle size was so experimentally confirmed to be 0.1 μm. The particles were spheres shaped in aqueous solution. The mixture was prepared in a plastic tank before being used into the setup tank. The 3 liters of water were divided in smaller amount of water inserting the fixed ratio of particle solution to obtain a concentration of 1%. They were in the end mixed together and inserted into the setup tank.
Three different measurements were made with a drop of the sample in a distilled water aqueous solution. The histogram and the different measurements show a good quality of the particles (Figure 6.4, Figure 6.5).

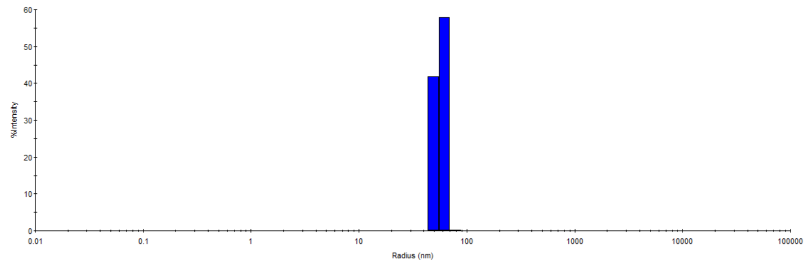

Figure 6.4: Histogram of the mean particle size for the 0.1 micron latex particles

In a first moment the setup was used just with pure water in order to check the clean membrane resistance and the permeability value, increasing the TMP through the pump settings from 10% to 70% of the pump speed.
The second set of experiments used water with particle concentration of 1% as previously described and pump speed set at 50% in order to have a constant feed flow and TMP (trans membrane pressure).
A sample of the permeate flow was measured every 10 minutes to check the flux decline due to pore gel cake layer on the membrane. After a certain amount of time,

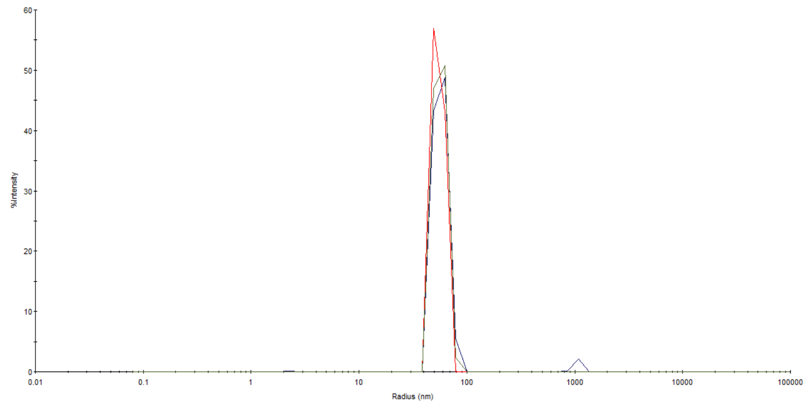

Figure 6.5: Three measurements for estimation of the size of the 0.1 micron latex particles

the flux became steady reaching its minimum permeate flux. The experiments was stopped when the steady state was achieved.
The last experiment showed the increase into the TMP needed to have a constant permeate flux during the time.

6.3.3 Results

During the experiments there was a pump malfunctions which limited the experimental time, so unfortunately was not possible to have more series of experiments for the second experiment previously mentioned.
Reparation of the pump was made by myself with the support of a university technician. The pump rotor was not spinning because of a high friction due to too tighten screw. The pump is currently working.
The feed flow was higher than what was in the initial intentions. In fact, with a small feed flow and a consequent small shear rate , it would have been possible give more focus the importance of this parameter from a small to a higher value
Table 6.3 summarizes the input while, table 6.4 summarizes the experimental results.

The feed flow was kept constant at 250 L/h, the same for the TMP which

Volumetric Feed Concentration	TMP	Membrane Resistance	Shear rate
1%	1.6 bar	1.45e12	5000 s^{-1}

Table 6.3: Matlab Simulation input

Time(min)	0	15	25	45	75	95	125	165	185
Permeate Flux(L/h)	1.5000	1.2800	1.2400	1.0200	0.9200	0.8000	0.8000	0.8000	0.8000

Table 6.4: Experimental Permeate Flow vs Time

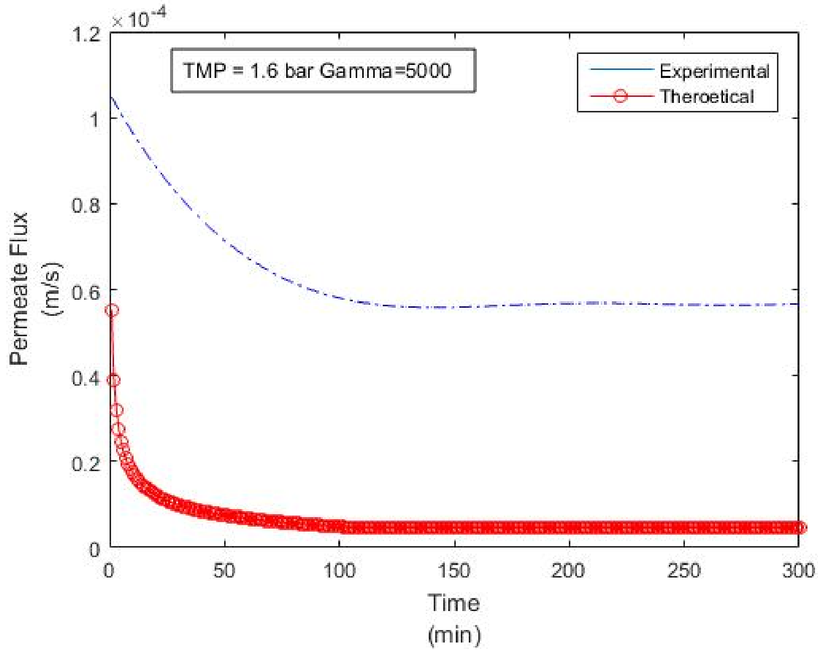

Figure 6.6: Experimental vs Theoretical Permeate Flux

was approximately 1.45 bar. The figure 6.6 shows the plot with both theoretical and experimental data.
The experimental data compared to the theoretical gives a lower steady flux, this could be due to a lower feed concentration value since most of the particles tended to float on the top of the tank, while the actual feed was taken from the bottom. The capillar dimensions of the membrane could actually create problem to the formation of a cake layer gel and this would be another possible factor in the dif-

ference between the model and the experiments.
The Matlab script for the comparison with the experimental data is included in Appendix C.
Even if there is a big difference between experimental and theoretical data, it is reported in different papers a difference up to 2 order of magnitude between experimental and theoretical data [20], so the model can show an interesting dependence of the steady state and time to reach it with the shear rate.

Chapter 7

CFD Simulations

In this chapter different CFD simulations will be presented. Computational Fluid Dynamic is a branch of fluid mechanics which uses numerical methods and algorithm to solve fluid dynamic problems. The interaction between the fluids and the boundary conditions are performed by computers with the support of 2D or 3D geometry describing the problem and its division in small computational cells (Mesh).
To simplify the calculation of our problem, a simpler geometry is used: a 2D model with a symmetry axis which will reduce the computational time compared to a whole 3D model. Also some simulations will be conducted on a larger diameter.
The reason of using a larger pipe diameter is to stay closer to real cases of reasonable two-flow injection use. In order to have some enhancement the the air should be injected in the center of the pipe and create a thin film of liquid near the wall. The air should stay in the center, far from the membrane area, so that the just the liquid can be filtrated. This would be impossible into a capillar pipe, like the one of the experimental setup.
The ratio of air will be chosen in order to stay into a slug flow, which is easily achievable and being a discontinuous flow would give a shear stress with some frequency profile which is found to have the highest impact on fouling decrease.
The values of the shear rate for different ratios air/water will be inserted into the model to verify the enhancement on the steady state, keeping the water value

constant.

7.1 Geometry

Different geometries were created for the different simulations. A first geometry was used to verify the permeate flux with clean water use.
The geometry 1 (Figure 7.1) is a representation of the experimental setup for clean water. The length is 250 mm, with porous zone height 2.5 mm and the same for the fluid zone, which will be just half of it for the symmetry.
The two different colour into the model represents two different material zones. The upper one is the porous zone, while the lower one is the effective channel of the pipe. The Boundary conditions to close the Reynold's Equarionts were : Velocity Inlet, Crossflow pressure outlet and pressure outlet.

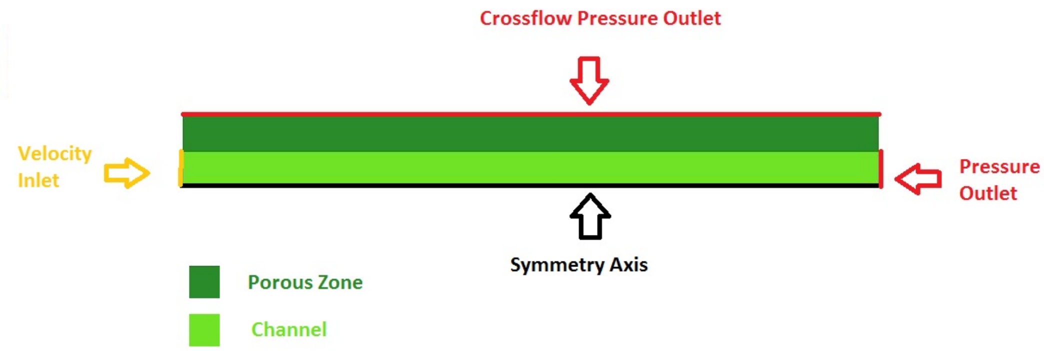

Figure 7.1: Geometry number 1 and its Boundary conditions

The geometry 2 (Figure 7.2) is a representation of the experimental setup in hypothesis of 2-phase flow. The length is 250 mm, with 3 different material zones: porous zone, liquid inlet and gas inlet. The geometry will be the similar to the one previously described but the fluid zone will be divided in two parts.
The Boundary conditions to close the Reynold's Equations were : Velocity Inlet,

Crossflow pressure outlet, and pressure outlet.
The geometry number 3 (Figure 7.3) will be larger than experimental membrane

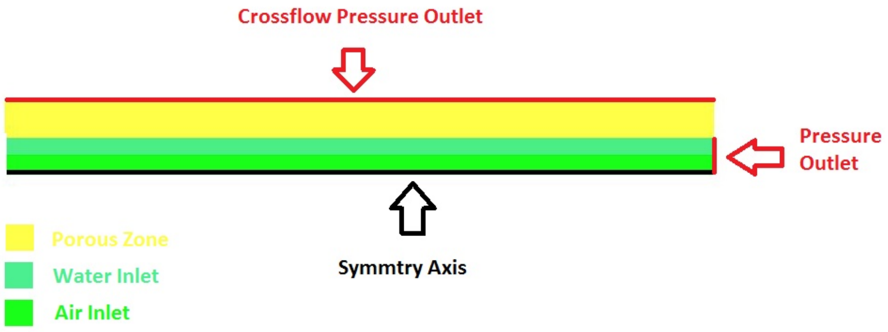

Figure 7.2: Geometry number 2 and its Boundary conditions

setup. This will make computational calculation easier and also will be more adapt to the aim of this thesis where the air injection should be in the center of the pipe. This is impossible to achieve in a capillar flow and the air in contact with wall would decrease the permeate flow. In order to achieve this a larger diameter pipe is required. The dimensions are: radius 50 cm and length 200 cm. The porous zone is substituted by a wall.

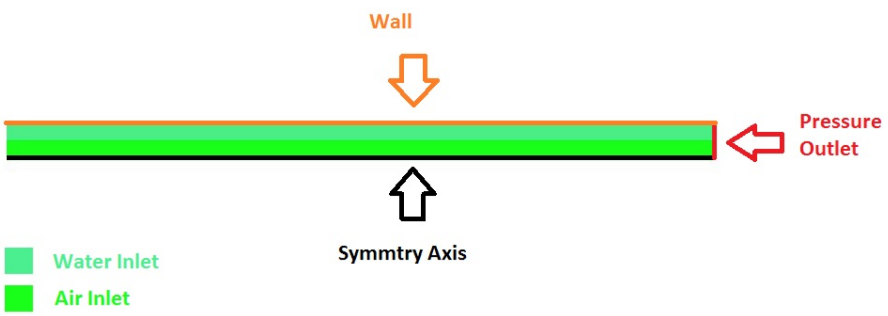

Figure 7.3: Geometry number 2 and its Boundary conditions

7.1.1 Mesh

All the three figures were meshed using Map scheme. For their simple geometry, this kind of scheme would give the least skewness and the more reliability in the calculations.
The number of elements for Geometry 1, 2 and 3 is summarized in the table.

Geometry	1	2	3
Number of elements	125000	125000	300000

Table 7.1: Number of elements in the mesh for the different geometries

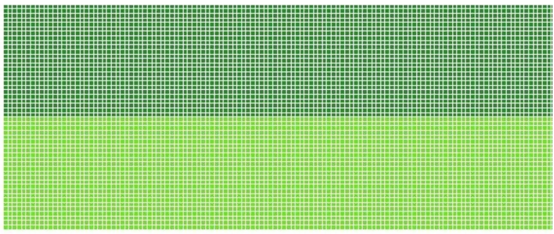

Figure 7.4: Zoom on part of the geometry mesh.

7.2 Permeate Flow

The aim of the following simulation is to insert similar boundary conditions to the experimental one (Velocity inlet, Pressure Outlet, Permeate Pressure Outlet) and simulate a flow inside a porous zone. Two inputs are required for this kind of simulations: the permeability which has been previously obtained experimentally and the porosity.
The model should give an accurate value of the permeate flow in a single-phase flow and be comparable with the experimental one. Based on this result it would be possible to do further simulations with a two-phase flow. The fouling particles

will not be included into the two-phase flow which will include just air injections. The permeate flow could anyway increase due to the higher shear stress not for the decrease of cake layer but because of another effect due to high shear stress: increasing mass transfer coefficient.
7.2.
The output values of the simulations are similar to the experimental one and can

Velocity Inlet	**Pressure Outlet**	**Inertial Viscosity (1/Permeability** m^2	**Porosity**
5.68 m/s	0.66 bar	5.8e14	0.46

Table 7.2: Boundary Conditions as simulation input

overall be considered very good (Table 7.3. The wall shear stress could not be included into the output since, the method used in Fluent to simulate a porous zone does not use walls and so can not take in account this output. To obtain this value a new simulation was made with a simple pipe, which can be considered good for evaluating the shear stress because the permeate flux is less than 10% of the feed.
This value gave good correspondence to the standard calculation for a single phase flow shear rate in a pipe:

$$\gamma = \frac{8v}{d} \tag{7.1}$$

Where:

γ = Shear rate
v = Fluid Velocity
d = Pipe Diameter.

7.3 Two-phase flow with porous zone

Once verified the reliability of the defined porous zone with the previous experiment, as mentioned in the previous section, a simulation for a two-phase flow to

	Permeate Flow	Pressure inlet
Experimental	0.00037 kg/s	0.87 bar
Simulation	0.00028 kg/s	0.78 bar

Table 7.3: Experimental vs Simulation Outlet

check if the expected increase into the shear stress would correspond to a higher permeate flux.
This simulation unlikely the model presented in Chapter 5 does not take into account fouling, so it is just to check if the shear stress/shear rate increase could beside decrease the fouling effect give enhancement in permeate flux through an increase in the mass transfer coefficient.
Leveque type equation in fact describes the mass transfer coefficient in a membrane as :

$$k = 1.62\left(\frac{\gamma D^2}{L}\right)^{1/3} \tag{7.2}$$

Unfortunately Fluent in order to calculate a porous zone and the relative permeate flux (dependent on k) "simulates" sinks into a liquid zone with magnitude proportional to the viscous resistance. This does not take into account then the value of the shear rate.

7.4 Two-Phase Flow

For all the two-phase flow simulations the water inlet was set constant and the air injection as variable parameter. Through the map presented in Chapter 4 for vertical pipes, the boundary inlet conditions for the air phase were chosen in order to have a slug flow.
The water inlet was 200 kg/s for all the simulations. Based on the dimensions of Geometry number 3 previously described the air injection should lie in the range 0- 1.5 kg/s to have a slug flow.

The settings for the simulations were: mixture multiphase model , and k-ϵ for the turbulence, gravity vector was chosen in order to have gravity acting against the flow into the membrane.
Mixture model is the least accurate model among the three options provided by Fluent, but a multiphase simulation is a function of time. This means that is not possible to choose a long time step or the simulations will not converge to a solution.
Even a few seconds of simulations could take more than 8 hours with the mixture model which is the least "computational-demanding".
Even if the simulation was not very long, the results hereby obtained from the simulations can be considered valuable since the first air bubbles reaches the end of the membrane. Even if the results are dependent on the time they start have periodically value and different from the inital transient values.
The superficial tension was set as constant: 72 dyn/cm between water and air.
The very first simulation was executed for a single-phase flow to check the mean shear stress value and compare it later with the 2-phase simulations.
The reference value for is 2 Pa for the wall shear stress (Figure 7.5) , which corresponds to a Shear Rate of 2247 s^{-1}.

7.4.1 Simulation with 0.1 m/s

The first simulation used a very low velocity/mass flow inlet. The conditions are similar to those introduced in the beginning of the sections. The simulation time was stopped when the air reached the outlet of the channel.

The figure 7.6 show a pattern that is not properly a slug, since the water bubble never attach together. The shear stress was plotted as function of the wall length in figure 7.7.
The shear stress in the whole membrane is almost everywhere higher than the 1-phase simulation with the same mass flow input
The first part of the membrane could be not reliable since the flow is not yet

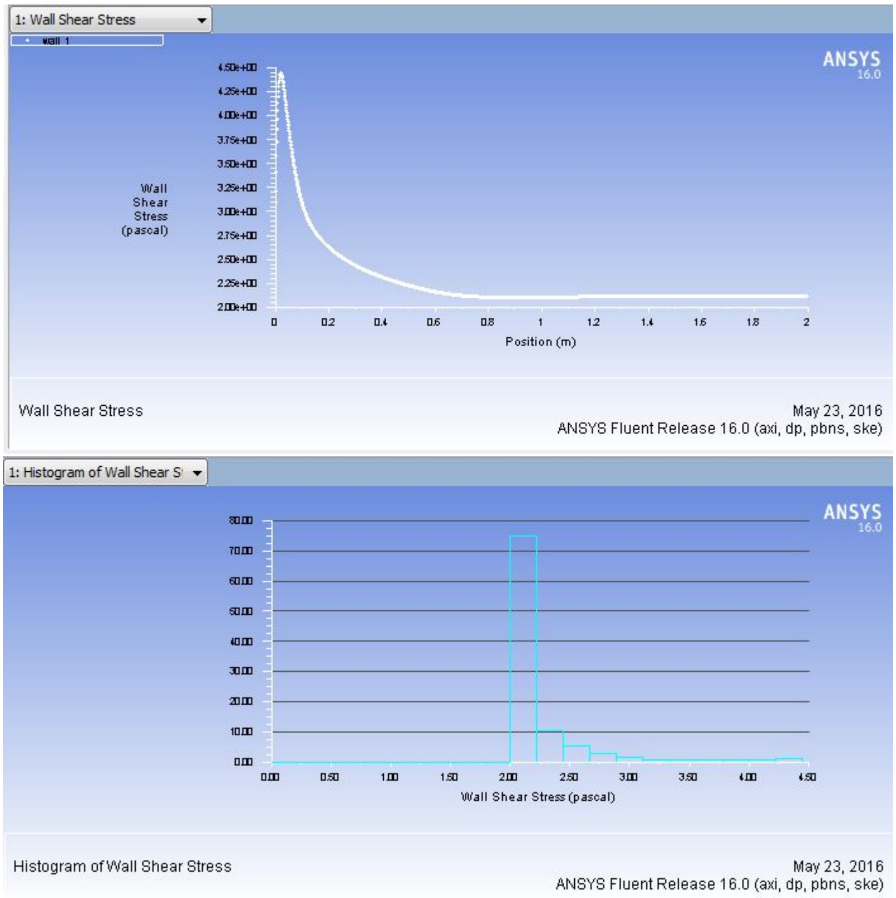


```
0 elements between 1.7790485 and 2.0014296 (0 %)
1499 elements between 2.0014296 and 2.2238107 (74.95 %)
208 elements between 2.2238107 and 2.4461917 (10.4 %)
110 elements between 2.4461917 and 2.6685728 (5.5 %)
57 elements between 2.6685728 and 2.8909539 (2.85 %)
31 elements between 2.8909539 and 3.1133349 (1.55 %)
19 elements between 3.1133349 and 3.335716 (0.95 %)
14 elements between 3.335716 and 3.5580971 (0.7 %)
13 elements between 3.5580971 and 3.7804781 (0.65 %)
12 elements between 3.7804781 and 4.0028592 (0.6 %)
12 elements between 4.0028592 and 4.2252403 (0.6 %)
25 elements between 4.2252403 and 4.4476213 (1.25 %)
0 elements above 4.4476213 (0 %)
```

Figure 7.5: Wall shear stress in 1 phase flow

developed.
The histogram (Figure 7.8) shows the distribution of the shear stress.
A value of 3 Pa can be considered as average for this simulation.

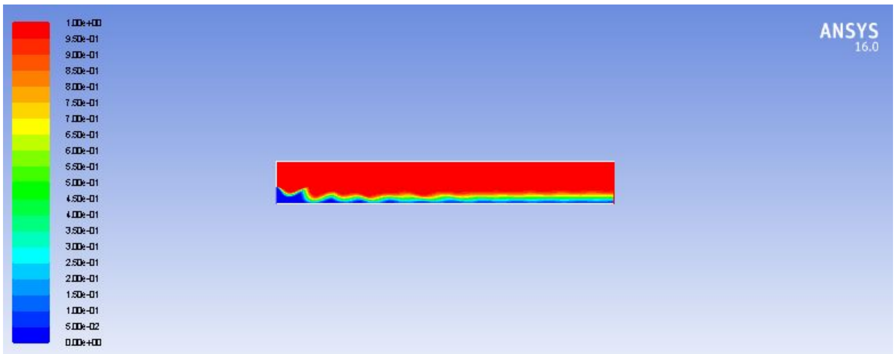

Figure 7.6: Gas Phase Graph in the symmetrical 2D pipe with air injection of 0.1 m/s

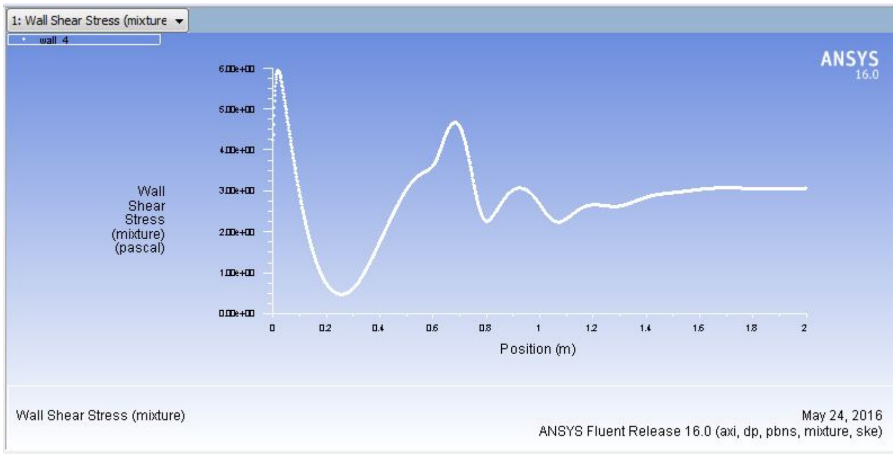

Figure 7.7: Gas Phase Graph in the symmetrical 2D pipe with air injection of 0.1 m/s

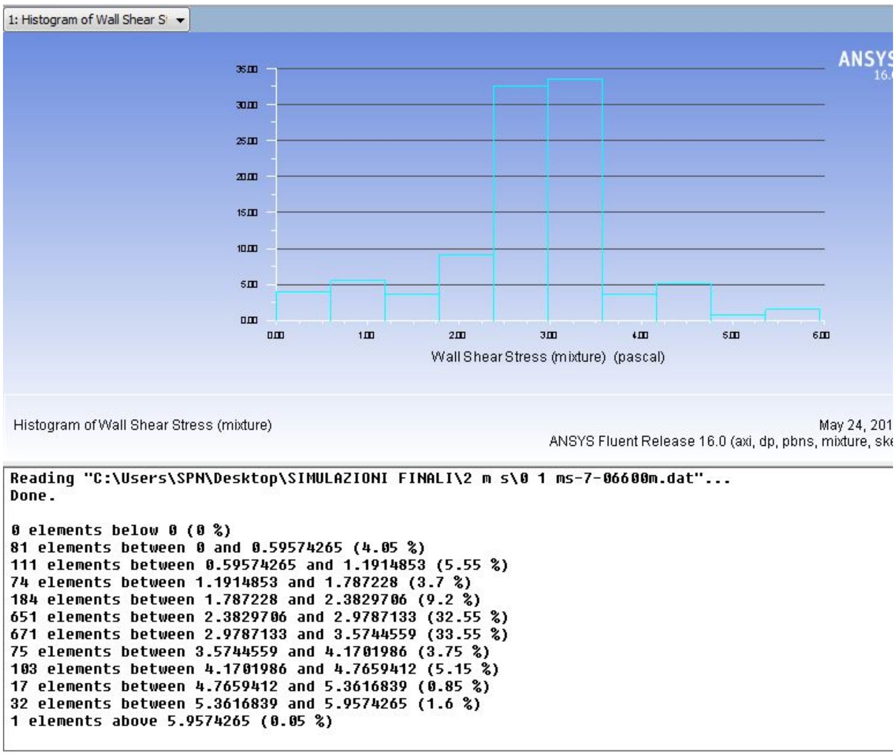

Figure 7.8: Shear Stress distribution into the membrane

7.4.2 Simulation with 1 m/s

The second simulation used velocity of 1 m/s. The mass flow inlet is still very low but the slug range is very wide and to meet real application, a low air velocity injection is required. The shear stress was plotted as function of the wall length (Figure 7.9). This plot is of course a function of the stop time of the simulation. This means that the peaks are expected reach all the membrane length at different time. The peak value of 5.5 Pa can be considered then as value of the shear stress, with a certain frequency. Which has been experimentally considered the best profile to avoid fouling. This kind of profile, as explained in Chapter 3, gave better results compared with a constant profile with the same magnitude. For this reason considering the value of the peak as value of the whole channel shear stress would put us in "safe" conditions, since empirically they should have even better results in the flux time decline performances.

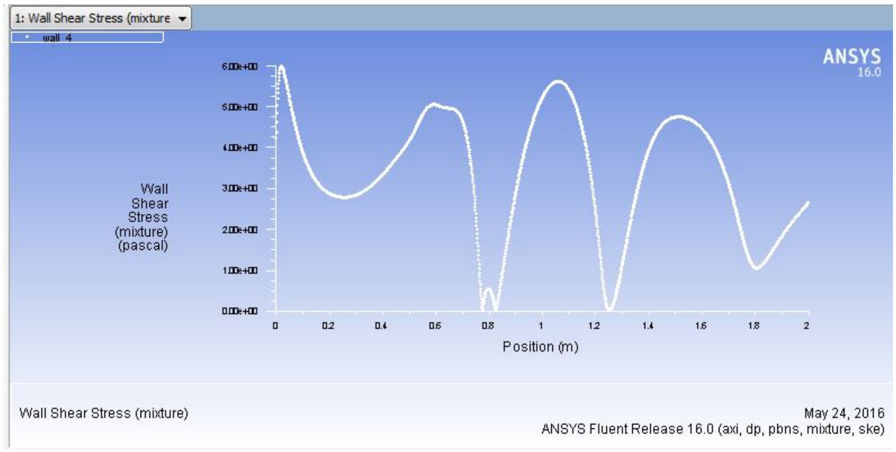

Figure 7.9: Shear stress profile for an air injection 1 m/s

The shear stress follows a sinusoidal trend, which is good for the shear stress because it has been experimentally proven to be more effective. The highest peak is around 5.5 Pa.

7.4.3 Simulation with 2 m/s

This simulation gave a very similar results and plot with the 1 m/s one. The high shear stress peak was barely higher.

7.4.4 Simulation with 4 m/s

A simulation with an input velocity of 4 m/s gave a similar profile but with a peak value of 30 Pa.

7.4.5 Results and Discussion

A summary chart with the simulation input/output values is presented: The Shear

	Water Velocity Inlet	**Air Velocity Inlet**	**S**hear Stress Peak
Simulation 1	1.2 m/s	0 m/s	2 Pa
Simulation 2	1.2 m/s	0.1 m/s	4 Pa
Simulation 3	1.2 m/s	1 m/s	5.5 Pa
Simulation 4	1.2 m/s	2 m/s	6 Pa
Simulation 5	1.2 m/s	4 m/s	30 Pa

Table 7.4: Boundary Conditions as simulation input

stress value presented higher value in all the simulations compared to the original one. This difference , even if it is not so big, creates an high difference in the shear rate values which will be the one evaluated into the model.
Another curiosity is the not proportionality between difference value of air inlet. This could be explained with the slug motion, which tend to attract together air bullet and not in a continuous way.

Chapter 8

Results and Discussion

In the following chapter, the shear rate stress obtained through CFD simulations is inserted into the Matlab script describing the flux decline model introduced in Chapter 5.
The curves will be compared for the exact same conditions, underlining eventual enhancement of the flux. After this evaluation, the boundary conditions will be changed in order to evaluate the best conditions for the air injection

8.1 Results

The table 8.1 summarizes the results from the model for the different simulations with the same input as in Fluent.

	Air Velocity Inlet	Shear Rate	Steady State Flux	Steady State Time (min)
Simulation 1	0 m/s	2247 s^{-1}	1.8222 10^{-6} m/s	273 min
Simulation 2	0.1 m/s	4494 s^{-1}	2.295 10^{-6} m/s	173 min
Simulation 3	1 m/s	6180 s^{-1}	2.5531 10^{-6} m/s	140 min
Simulation 4	2 m/s	6742 s^{-1}	2.62 10^{-6} m/s	132 min
Simulation 5	4 m/s	33708 s^{-1}	4.49 10^{-6} m/s	46 min

Table 8.1: Results of different simulations with Flux Decline model

8.1.1 Air injection 0.1 m/s

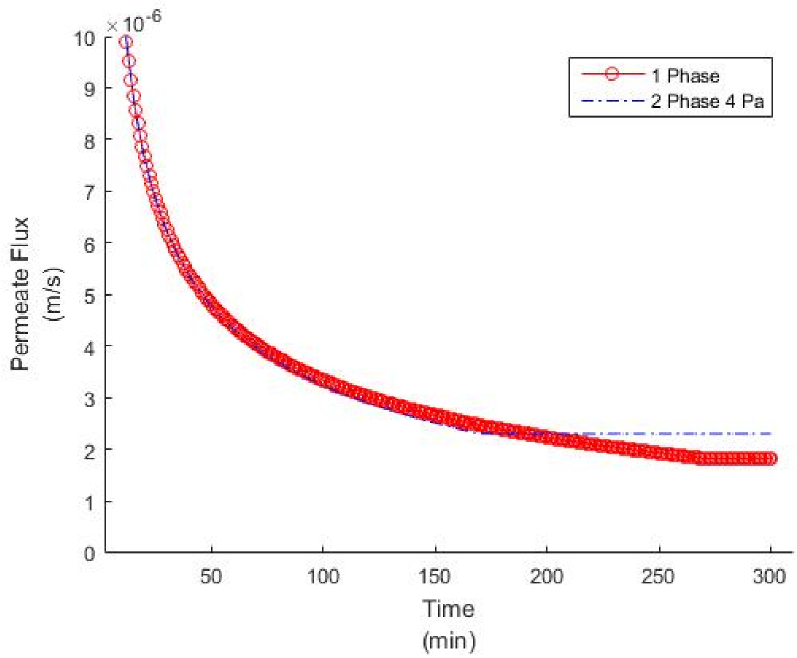

Figure 8.1: Flux Decline comparison between 1 phase flow and 2 phase flow with air injection at 0.1 m/s

The curves follow the same trend when filtration starts but the 2 phase flow reaches its steady flow earlier.
The value for the steady flux of the two-phase flow is almost 25% higher than the value of the steady state for the one-phase.
Observing the graph, the potential advantage is the possibility of having an higher flux when the steady state is reached. Theoretically this would not bring any advantage in case both the membranes would be changed at the same time (the time the first one reaches the steady state) but this can be very useful if this is not always possible and the time for reaching the steady state is short.

8.1.2 Air injection 1 m/s and 2 m/s

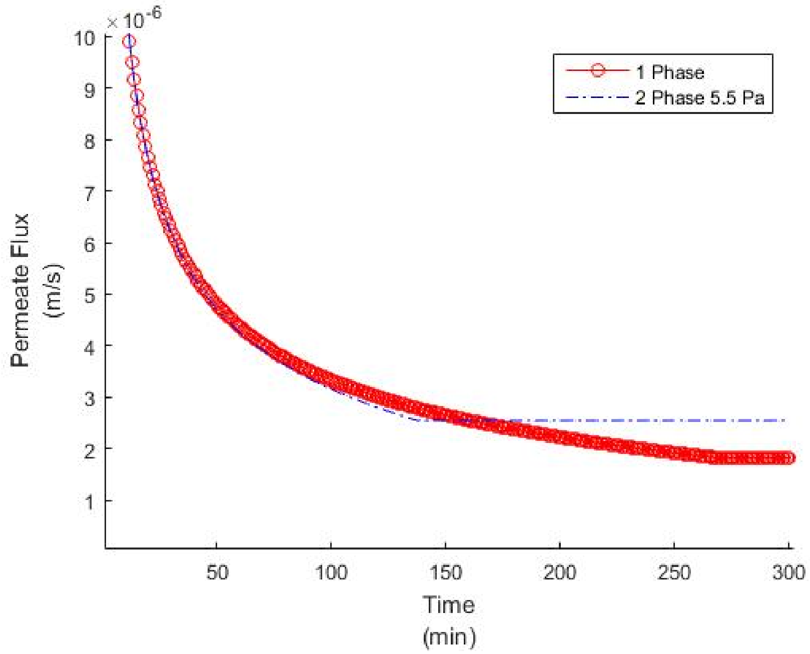

Figure 8.2: Flux Decline comparison between 1 phase flow and 2 phase flow with air injection at 1 m/s

The steady permeate flux with 1 m/s is 40% higher compared with the 1 phase flow. The increase into the velocity is about 10 times, while the flux does

not have a proportional benefit. This means that a small injection could be enough to increase the permeate flux and still keep the energy consumption low.
Similar results are obtained for an air injection of 4 m/s. The enhancement is about 44% . Just for 4% than with double the injection of air.

8.1.3 Air injection 4 m/s

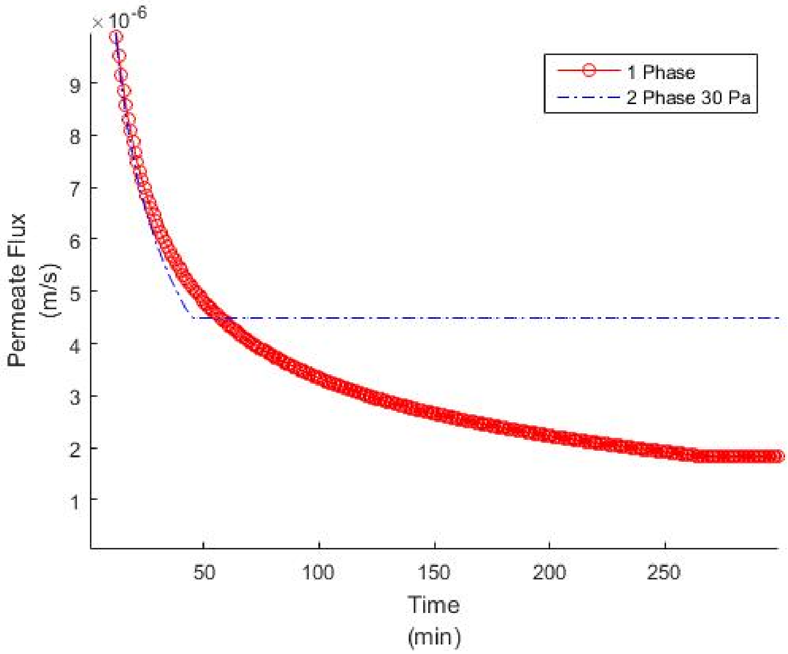

Figure 8.3: Flux Decline comparison between 1 phase flow and 2 phase flow with air injection at 4 m/s

The flux enhancement is 146 %. This means that over a certain flow mass input a new pattern in the two phase flows develop and creates better conditions.

8.2 Optimal conditions for the two phase-flow enhancement

With the model as Matlab script it is easy to change the input parameters and find out in which cases an increase of shear stress would bring more benefits.
In order to study this, the membrane and flow boundary conditions were changed, comparing two different flows with a fixed ratio of shear rate.
A defined ratio between two shear rate values corresponds to a constant ratio in both the steady state flux and time to reach it.
Comparing two different simulations with different shear rates, it is possible to observe that the curve follows more or less the same trend before the one with the higher shear stress reaches the steady state. The simulation with a lower shear rate will continue to decrease.
This means that an higher shear stress is particularly useful when the time to reach the steady state in one phase flow is very long. In fact considering a backflush operation for both the systems when the slowest steady state is reached, the difference into the time to reach it and , and the difference into the steady states flux will give a much higher volume of filtered water in the simulation with a higher shear rate.
The parameters that increase the time to reach the steady state are: longer membrane length, higher TMP, higher feed concentration, smaller fouling particles. A membrane filtration with air injection then, would be more efficient in terms of volume of filtered water/time when the system has these characteristics.

Chapter 9

Conclusions

A real prediction on produced water enhancement could be hard to obtain since its composition (feed concentration, particle size) can be very different, not constant and very dependent on the extraction zone.
The size distribution of the oil particles in produced water is very large, as illustrated into Figure 9.1.
Usually the droplets size exceeds 0.1 μ m and may be larger than 100 μ m. The theoretical model requires as input the particle size which is of course not always possible to find out, but from the simulations and Matlab script it is possible to observe a big enhancement through the use of air injection into the system. Anyway from the simulations, experiments and the Matlab scripts it is possible

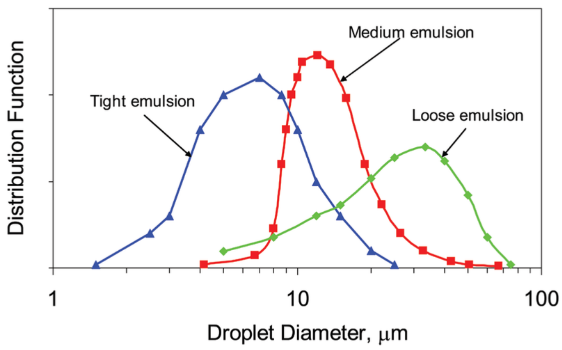

Figure 9.1: Particle Size distribution for oil droplets[21]

to observe that air injection inside a membrane could be a very useful technique, which could bring benefit in the quality of water, performance of the membrane and time saved into the production avoiding continuous production stop for maintenance operation.
This technology is already in use but not so much is reported about the performances and their possible optimization.
The results show an enhancement until 150% in the permeate flux, and still an impressive increase of about 45% for small flow air injections, which could be easier to achieve.
This technology needs of course specific geometries and conditions to give its best, but its development could allow to have the same results with less energy consumption, reducing the total fouling particles on the membrane, avoiding the cake layer formation and making the lifetime of a membrane longer.

Bibliography

[1] Jerry Neff Kenneth Lee. *Produced Water: Environmental Risks and Advances in Mitigation Technologies*. Springer Science, 2011.

[2] M. Al-Marri C.Clarkin S. Watson A. Ahmed S. Bach S. Judd, H. Qiblawey. The size and performance of offshore produced water oil-removal technologies for reinjection. *Separation and Purification Technology*, 2014.

[3] Simon Judd. *The MBR Book - Principles and Applications of Membrane Bioreactors for Water and Wastewater Treatment*.

[4] Filtration. `http://www.filtsep.com/view/30721/membranes-expanded-ptfe-finds-new-markets/`.

[5] Gea company website. `http://www.gea.com/global/en/binaries/general-membrane-filtration_tcm11-17109.pdf`.

[6] Crossflow vs dead-end filtration. `http://www.cleanflowfilter.nl/ceramic-membrane-filter/`.

[7] Pyramid flow diagram image. `http://www.membranes.com/docs/trc/flowcon.pdf`.

[8] Myoung Jun Park Ho Kyong Shon 2 Jihye Kim, Kwanho Jeong and Joon Ha Kim. Recent Advances in Osmotic Energy Generation via Pressure-Retarded Osmosis (PRO): A Review.

[9] H. Doan A. Abdelrasoul and A. Lohi. Fouling in Membrane Filtration and Remediation Methods.

[10] Henrik Bank Madsen Kristofer Gjendal. *Flow in Microporous Silicon Carbide: an Experimental and Numerical Study.*

[11] Yiwei Wang Hsin-I Chang. *Cell Responses to Surface and Architecture of Tissue Engineering Scaffolds.*

[12] Yu Boming Xu Peng. *Developing a new form of permeability and Kozeny–Carman constant for homogeneous porous media by means of fractal geometry.*

[13] Qiang Zhang Wojciech Sobieski. *SENSITIVITY ANALYSIS OF KOZENY-CARMAN AND ERGUN EQUATIONS.*

[14] *Carman PC. Fluid flow through granular beds. Trans Inst Chem Eng 1937;15:150–67.*

[15] Dionysios D. Dionysiou Daniel B. Oerther George A. Sorial Hyeok Choi, Kai Zhang. Influence of cross-flow velocity on membrane performance during filtration of biological suspension.

[16] E.R. Hall C.C.V. Chan, P.R. Bérubé. Relationship between types of surface shear stress profiles and membrane fouling.

[17] P.B. Whalley. *Two Phase Flow and Heat Transfer.*

[18] D.S. Pepper Q.Y. Li, Z.F. Cui. *Effect of bubble size and frequency on the permeate flux of gas sparged ultrafiltration with tubular membranes.*

[19] Lianfa Song. *Flux decline in crossflow microfiltration and ultrafiltration: mechanisms and modeling of membrane fouling.*

[20] GREG FOLEY. *Membrane Filtration A Problem Solving Approach with MATLAB.*

[21] droplet. `http://petrowiki.org/Oil_emulsions#Droplet_size_and_droplet-size_distribution`.

Chapter 10

Appendix

10.1 Appendix A - Permeability and Clean Membrane Resistance

```
clc
clear all
A = [0 0.065 0.225 0.455 0.765 1.115 1.4];          %TMP
B = [0 0.1204 0.4104 0.8364 1.3548 1.855 2.155];    %Permeate Flux
A=A*10^5;                                           %Pascal Conversion
B=(B/3600)*10^-3;                                   %m^3/s conversion
my_poly=polyfit(A,B,1);

scatter(A,B)
xlabel({'TMP','(Pa)'})
ylabel({'Qp','(m^3/s)'})
hold on
X2= 0:10000:150000; % X data range
Y2=polyval(my_poly,X2);                             %Linear fitting of the data
plot(X2,Y2)
figure
mu= 8.94*10^(-4);
```

```
w=0.0025;                                              %Wall thickness
dc=0.005;                                              %Inner diameter
L=0.25;                                                %Channel Length
Am=2*pi*0.003*0.25;                                    %Membrane Area
Rm=A./(mu*(B./Am));                                    %Membrane Resistance
scatter(A,Rm)
xlabel({'TMP','(Pa)'})
ylabel({'Membrane Resistance','(1/m)'})
k=my_poly(1)*mu*log(1+(2*w/dc))/(2*pi*L);          %Permeability of the membrane
```

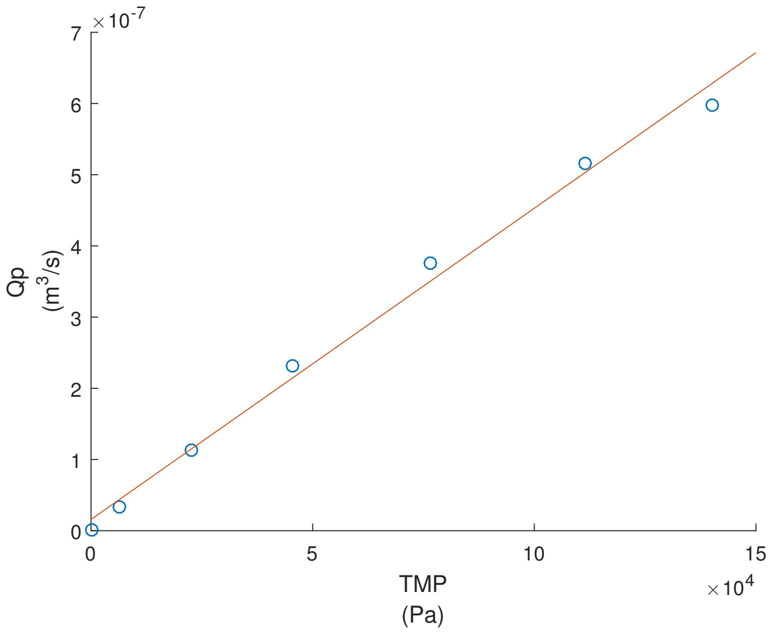

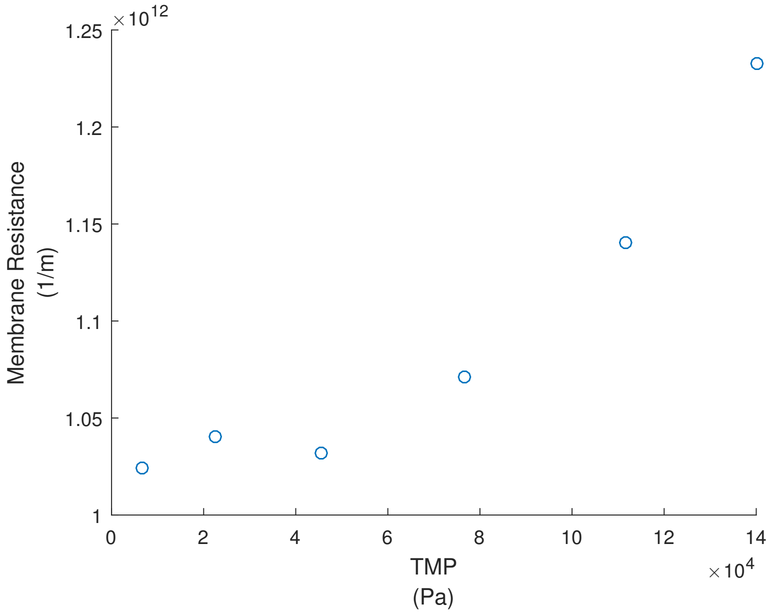
×10^12
1.25
1.2
1.15
1.1
1.05
1
Membrane Resistance
(1/m)
0
2
4
6
8
10
12
14
TMP
(Pa)
×10^4

10.2 Appendix B - Flux Decline Model

```
clc
clear all
syms x
mu=8.9*10^-4;                    %Water Viscosity
c0=0.01;                        %Feed Concentration
cg=0.52;                         %Cake Concentration (Volume Fraction)
%cg=(1+((L*Vlim^3)/((1.31^3)*(D^2)*gamma)))*c0;
epsilon=1-cg;                    %Porosity of Cake Concentration
gamma=100;                       %Shear Rate
ap=0.05*10^-6;                   %Particle Radius
Vlim=1.89*10-6;                  %Steady experimental velocity
constant=45;                     %Constant for Carman Kozeny
k=1.38064852*10^-23;             %Boltzmann constan
Dp=159000;                       %TMP
T=293;                           %Temperature
L=0.25;                          %Length of Membrane
Nfc=15;                          %Filtration number
Rm=2.4*10^8;                     %Membrane Resistance*viscosity
D=k*T/(6*pi*mu*ap);              %Diffusion Coefficient with Stoke Einstein eq.
Dpc=3*k*T*Nfc/(4*pi*ap^3);       %Critical pressure for fouling
timend=60*300;                   %Simulation time end

cg=0.52;
rc=(constant*mu*(1-epsilon)^2)/((ap^2)*(epsilon^3));
%Specific cake resistance with Carman Kozeny
Vsteady=1.31*(((gamma*D^2)/L)^(1/3))*((cg/c0)-1)^(1/3);
%Average permeate flux in steady state over the whole channel at steady state
tss1=(L/(gamma*(D^2)))^(2/3);
tss2=(c0/(cg-c0))^(2/3);
tss3=(cg/c0);
```

```
tss4=(Dp-Dpc)/rc;
tss=0.351*tss1*tss2*tss3*tss4;
%Time to reach the steady state in sec
tssmin=round(tss/60);
%Time to reach the steady state in minutes
veq=((2/3)^(1/3))*((((gamma)*D^2)/x)^(1/3))*((cg/c0)-1)^(1/3);
%Local equilibrium flux in function of x coordinate
veqint=int(veq,x);
C=0;

for t=1:1:timend/60;
    tt=t*60;
vt(t)=((Dp-Dpc)/Rm)*(1+(2*rc*(Dp-Dpc)*c0*tt/(cg*Rm^2)))^(-1/2);
X(t)=4.81*(D^2*gamma*2)*((cg/c0)-1)*((c0/cg)^(3/2))*(rc*tt/(Dp-Dpc))^(3/2);
Z=X(t);
Veqint(t)=subs(veqint,x,Z);
Vt(t)=(Veqint(t)+((L-X(t))*vt(t)))/L;
%Average permeate flux in steady state over the whole channel at time t
if Vt(t)>Vsteady
   Vt(t)=Vt(t);
else
    Vt(t)=Vsteady;
end
if t~=1
    if C==0 & Vt(t)==Vt(t-1)
        C=t;
    else
    end
end
end
if C~=0
    tssmin=C;
else
```

```
    tssmin=tssmin;
end
plot(Vt)
```

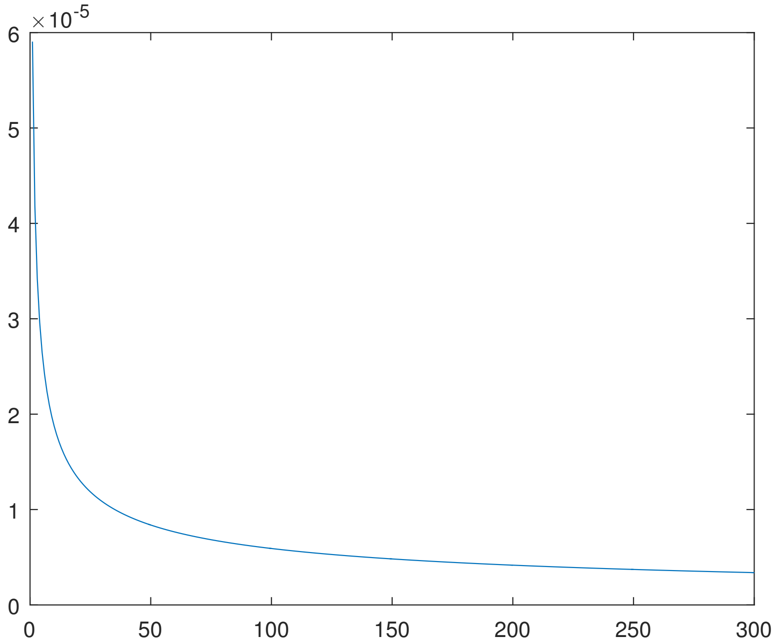

10.3 Appendix C - Experimental vs Theoretical Calculation

```
clc
clear all
syms x
mu=8.9*10^-4;                          %Water Viscosity
c0=0.01;                              %Feed Concentration
cg=0.52;                               %Cake Concentration (Volume Fraction)
%cg=(1+((L*Vlim^3)/((1.31^3)*(D^2)*gamma)))*c0;
epsilon=1-cg;                          %Porosity of Cake Concentration
gamma=5000;                             %Shear Rate
```

```
ap=0.05*10^-6;                      %Particle Radius
Vlim=1.89*10-6;                     %Steady experimental velocity
constant=45;                        %Constant for Carman Kozeny
k=1.38064852*10^-23;                %Boltzmann constan
Dp=139000;                          %TMP
T=293;                              %Temperature
L=0.25;                             %Length of Membrane
Nfc=15;                             %Filtration number
Rm=2.4*10^8;                        %Membrane Resistance*viscosity
D=k*T/(6*pi*mu*ap);                 %Diffusion Coefficient with Stoke Einstein equat
Dpc=3*k*T*Nfc/(4*pi*ap^3);          %Critical pressure for fouling
timend=60*300;                      %Simulation time end

cg=0.52;
rc=(constant*mu*(1-epsilon)^2)/((ap^2)*(epsilon^3));
%Specific cake resistance with Carman Kozeny
Vsteady=1.31*(((gamma*D^2)/L)^(1/3))*((cg/c0)-1)^(1/3);
%Average permeate flux in steady state over the whole channel at steady state
tss1=(L/(gamma*(D^2)))^(2/3);
tss2=(c0/(cg-c0))^(2/3);
tss3=(cg/c0);
tss4=(Dp-Dpc)/rc;
tss=0.351*tss1*tss2*tss3*tss4;
%Time to reach the steady state in sec
tssmin=round(tss/60);
%Time to reach the steady state in minutes
veq=((2/3)^(1/3))*((((gamma)*D^2)/x)^(1/3))*((cg/c0)-1)^(1/3);
%Local equilibrium flux in function of x coordinate
veqint=int(veq,x);
C=0;

for t=1:1:timend/60;
    tt=t*60;
```

```
vt(t)=((Dp-Dpc)/Rm)*(1+(2*rc*(Dp-Dpc)*c0*tt/(cg*Rm^2)))^(-1/2);
X(t)=4.81*(D^2*gamma*2)*((cg/c0)-1)*((c0/cg)^(3/2))*(rc*tt/(Dp-Dpc))^(3/2);
Z=X(t);
Veqint(t)=subs(veqint,x,Z);
Vt(t)=(Veqint(t)+((L-X(t))*vt(t)))/L;
%Average permeate flux in steady state over the whole channel at time t
if Vt(t)>Vsteady
   Vt(t)=Vt(t);
else
    Vt(t)=Vsteady;
end
if t~=1
    if C==0 & Vt(t)==Vt(t-1)
        C=t;
    else
    end
end
end
if C~=0
    tssmin=C;
else
    tssmin=tssmin;
end
plot(Vt)
hold
dc=0.005;
A= [75 64 62 51 46 40 40 40 40 40 40 40 40 40 40 40 40 40 40 40 40];
A=(A/(180*1000*1000))/(pi*dc*L);
B= [0 15 25 45 75 95 125 165 185 215 225 235 245 255 265 275 285 295 305 315 325];
my_poly=polyfit(B,A,7);
x=1:1:300;
y=polyval(my_poly,x);
plot(x,Vt,'-ro',x,y,'-.b')
```

```
legend('Theroetical','Experimental')
xlabel({'Time','(min)'})
ylabel({'Permeate Flux','(m/s)'})
```

```
Current plot held
Warning: Polynomial is badly conditioned. Add points with distinct X values,
reduce the degree of the polynomial, or try centering and scaling as described
in HELP POLYFIT.
```